ACI 228.2R-13

Report on Nondestructive Test Methods for Evaluation of Concrete in Structures

Reported by ACI Committee 228

American Concrete Institute®

First Printing
June 2013

American Concrete Institute®
Advancing concrete knowledge

Report on Nondestructive Test Methods for Evaluation of Concrete in Structures

The technical committees responsible for ACI committee reports and standards strive to avoid ambiguities, omissions, and errors in these documents. In spite of these efforts, the users of ACI documents occasionally find information or requirements that may be subject to more than one interpretation or may be incomplete or incorrect. Users who have suggestions for the improvement of ACI documents are requested to contact ACI via the errata website at www.concrete.org/committees/errata.asp. Proper use of this document includes periodically checking for errata for the most up-to-date revisions.

ACI committee documents are intended for the use of individuals who are competent to evaluate the significance and limitations of its content and recommendations and who will accept responsibility for the application of the material it contains. Individuals who use this publication in any way assume all risk and accept total responsibility for the application and use of this information.

All information in this publication is provided “as is” without warranty of any kind, either express or implied, including but not limited to, the implied warranties of merchantability, fitness for a particular purpose or non-infringement.

ACI and its members disclaim liability for damages of any kind, including any special, indirect, incidental, or consequential damages, including without limitation, lost revenues or lost profits, which may result from the use of this publication.

It is the responsibility of the user of this document to establish health and safety practices appropriate to the specific circumstances involved with its use. ACI does not make any representations with regard to health and safety issues and the use of this document. The user must determine the applicability of all regulatory limitations before applying the document and must comply with all applicable laws and regulations, including but not limited to, United States Occupational Safety and Health Administration (OSHA) health and safety standards.

Participation by governmental representatives in the work of the American Concrete Institute and in the development of Institute standards does not constitute governmental endorsement of ACI or the standards that it develops.

Order information: ACI documents are available in print, by download, on CD-ROM, through electronic subscription, or reprint and may be obtained by contacting ACI.

Most ACI standards and committee reports are gathered together in the annually revised *ACI Manual of Concrete Practice* (MCP).

American Concrete Institute
38800 Country Club Drive
Farmington Hills, MI 48331
U.S.A.
Phone: 248-848-3700
Fax: 248-848-3701

www.concrete.org

ISBN-13: 978-0-87031-820-7
ISBN: 0-87031-820-9

ACI 228.2R-13

Report on Nondestructive Test Methods for Evaluation of Concrete in Structures

Reported by ACI Committee 228

Michael C. Forde, Chair

Bernard H. Hertlein, Secretary

Muhammed P. A. Basheer
Jacob K. Bice
Andrew J. Boyd
Michael Brown
Honggang Cao
Nicholas J. Carino
William Ciggelakis
Neil A. Cumming
Aldo De La Haza
Ethan C. Dodge
Boris Dragunsky
Christopher C. Ferraro
Frederick D. Heidbrink
Kal R. Hindo
Robert S. Jenkins
Keith E. Kesner
H. S. Lew
Malcolm K. Lim
Kenneth M. Lozen
Larry D. Olson
Stephen Pessiki
John S. Popovics
Randall W. Poston
Paul L. Siwek
Patrick J. E.Sullivan

Consulting members
John H. Bungey
Hermenegildo Caratin
Gerardo G. Clemena
Al Ghorbanpoor
Alexander M. Leshchinsky
V. M. Malhotra
Claus G. Petersen
George V. Teodoro

Allen. G. Davis (deceased) made many contributions to this report.

A review is presented of nondestructive test (NDT) methods for evaluating the condition of concrete and steel reinforcement in structures. Methods discussed include visual inspection, stress-wave, nuclear, measurement of fluid transport properties, magnetic and electrical, infrared thermography, and ground-penetrating radar. The principle of each method is discussed and the typical instrumentation described. Testing procedures are summarized and the data analysis methods explained. The advantages and limitations of the methods are highlighted. This report concludes with a discussion of planning a NDT program. General information is provided for those faced with the task of evaluating the condition of a concrete structure and who are considering the applicability of NDT methods to aid in that evaluation.

Keywords: covermeter; deep foundations; half-cell potential; infrared thermography; nondestructive testing; polarization resistance; radar; radiography; radiometry; stress-wave methods; transport properties; visual inspection.

CONTENTS

ACI 228.2R-13 supersedes ACI 228.2R-98(04) and was adopted and published June 2013.

CHAPTER 1—INTRODUCTION

1.1—Scope

Nondestructive testing (NDT) methods are used to determine concrete properties and to evaluate the condition of concrete in deep foundations, bridges, buildings, pavements, dams, and other concrete construction. For this report, NDT is defined as generally noninvasive, with the exception of transport property tests, which may cause easily-repaired surface damage. While coring and load testing may be considered nondestructive, they are excluded from this report. Refer to ACI 437R for more information about strength evaluation of existing concrete buildings.

NDT methods are applied to concrete construction for four primary reasons:

1. Quality control of new construction
2. Troubleshooting problems with new and old construction
3. Condition evaluation of older concrete for rehabilitation purposes
4. Quality assurance of concrete repairs

NDT technologies are evolving and research continues to enhance existing methods and develop new methods. The report is intended to provide an overview of the principles of various NDT methods practiced and to summarize their applications and limitations. Emphasis is placed on methods that have been applied to measure physical properties other than the strength of concrete in structures, to detect flaws or discontinuities, and to provide data for condition evaluation. Methods to estimate in-place compressive strength are presented in ACI 228.1R.

1.2—Needs and applications

Nondestructive testing (NDT) methods are increasingly applied for the investigation of concrete structures. This increase in the application of NDT methods is due to a number of factors:

a) Technological improvements in hardware and software for data collection and analysis

b) The economic advantages in assessing large volumes of concrete compared with other methods

c) Ability to perform rapid, comprehensive assessments of existing construction

d) Specification of NDT methods for quality assurance of deep foundations and concrete repairs

An increased use of NDT methods is occurring despite the lack of testing standards for many of the methods. The development of testing standards is critical for proper application and expanded use of NDT methods for evaluation of concrete construction.

Traditionally, quality assurance of concrete construction has been performed largely by visual inspection of the construction process and by sampling the concrete to perform standard tests on fresh and hardened specimens. This approach does not provide data on the in-place properties of concrete. NDT methods offer the advantage of providing information on the in-place properties of hardened concrete, such as the elastic constants, density, resistivity, moisture content, and fluid transport characteristics.

Condition assessment of concrete for structural evaluation purposes has been performed mostly by visual examination, coring, and surface sounding, which refers to striking the object surface and listening to characteristics of the resulting sound. Condition assessments are used to examine internal concrete conditions and to obtain specimens for testing. This approach limits the areas of concrete that can be investigated effectively. Some coring may be necessary for calibration purposes, particularly if the concrete strength is required. Cores also cause local damage and limit the information to the core location. Condition assessments can be made with NDT methods to provide essential information for the structural performance of the concrete, such as:

a) Member dimensions

b) Location of cracking, delamination, and debonding

c) Degree of consolidation, presence of voids, and honeycomb

d) Steel reinforcement location and size

e) Corrosion activity of reinforcement

f) Extent of damage from freezing and thawing, fire, or chemical exposure

g) Strength of concrete

1.3—Objective

This report reviews the state of the practice for nondestructively determining nonstrength physical properties and conditions of hardened concrete. The overall objective is to provide the potential user with a guide to assist in planning, conducting, and interpreting the results of nondestructive tests (NDT) of concrete construction.

Chapter 3 discusses the principles, equipment, testing procedures, and data analysis of the various NDT methods. Typical applications and inherent limitations of the methods are discussed to assist the potential user in selecting the most appropriate method for a particular situation. Chapter 4 discusses the planning and performance of NDT investigations. Included in Chapter 4 are references to in-place tests covered in ACI 228.1R and other applicable methods for evaluating the characteristics of existing concrete.

CHAPTER 2—NOTATION AND DEFINITIONS

2.1—Notation

Because NDT crosses different science and engineering disciplines, the same symbols are used differently by different practitioners. The context of the symbol should be established and related to the body of text.

A = cross-sectional area (3.5.3, 3.6.2); wetted area (3.6.2)

A_c = shaft cross-sectional area (3.3.3, Appendix A)
B = magnetic induction (3.5.5)
B = constant in volts (3.5.4)
C = concentration (3.6.2); capacitance (3.5.4); electromagnetic wave speed (3.8)
C_b = bar wave speed (3.2, 3.3.1, 3.3.3); stress wave speed along the pile (Appendix A)
C_o = speed of light in air (3.8)
C_p = P-wave speed (3.2, 3.2.3)
$C_{R(f)}$ = surface wave speed of component with frequency f (3.2.4)
C_r = ratio of the R-wave speed to the S-wave speed (3.2)
C_s = S-wave speed (3.2, 3.2.2)
D = depth (3.2.3, 3.8); diffusion coefficient (3.5.3, 3.6.2); diameter (3.2.3)
D_p = diffusion coefficient of the ions through the pore fluid (3.5.3)
d = depth (3.2.1); diameter (3.3.1)
E = Young's modulus of elasticity (3.2); voltage (3.5.4); maximum acceptable error (4.2)
e = emissivity of the surface (3.7)
F = mass flux (3.6.2)
f = frequency (3.2.3)
G = shear modulus of elasticity (3.2)
H = magnetic field strength (3.5.5)
I = characteristic shaft impedance (3.3.3); amplitude of alternating current between outer electrodes (3.5.3); hydraulic gradient (3.6.2)
I_p = applied polarization current (3.5.4)
i = current (3.5.4)
i_{corr} = corrosion current density (3.5.4)
k = statistical factor (4.2); coefficient of permeability (3.6.2)
k_d = dynamic stiffness from mobility plot (3.2.5, 3.3.2; Appendix A)
L = length (3.3.1, 3.3.3, 3.5.3, Appendix A)
M_p = mass of pile (Appendix A)
m = mass (3.6.2)
N = average mobility (Appendix A)
n = sample size (4.2)
P = soil damping measure (Appendix A)
p_o = advance estimate of fraction defective (4.2)
Q = soil damping measure (Appendix A)
Q = flow rate (3.6.2); maximum amplitude in mobility plot of pile
R = rate of energy radiation per unit area of surface (3.7); reflection coefficient (3.2); electrical resistance in ohm (3.5.3, 3.5.4)
R_p = polarization resistance (3.5.4)
r = radius (Appendix A)
s = spacing between electrodes (3.5.3); sorptivity (3.6.2)
T = depth of reflecting interface (3.2.2); absolute temperature of surface (3.7)
t = travel time from transmitter to receiver (3.2.2); time (3.6.2, 3.8)
t_c = contact time (3.2.3)
V = volume of fluid absorbed (3.6.2); voltage (3.5.3)
V_d = wave speed in damaged concrete (3.2.1)
V_s = wave speed in sound concrete (3.2.1)
X = separation between transmitter and receiver (3.2.1, 3.2.2, 3.2.4)
X_o = distance at which the travel times for two wave paths are equal (3.2.1)
x = distance (3.6.2)
Z = specific acoustic impedance (3.2); depth (3.8)
α = signal attenuation (3.8)
β_s = the lateral soil shear wave velocity (Appendix A)
ε = dielectric constant (3.8)
ε_0 = dielectric constant of free space (air) (3.8)
ε_r = relative dielectric constant (3.8)
ϕ_f = phase angle of component with frequency f (3.2.4)
λ = wavelength (3.2.3)
λ_f = wavelength corresponding to component frequency (3.2.4)
μ = magnetic permeability (3.5.5)
ν = Poisson's ratio (3.2)
ρ = density (3.2); electrical resistivity of material (3.5.3)
$\rho_{1,2}$ = reflection coefficient (3.8)
ρ_c = density of shaft concrete (3.3.3, Appendix A)
ρ_s = soil density (Appendix A)
σ = conductivity (3.5.3, 3.8); the Stefan-Boltzmann constant (3.7); soil damping factor (Appendix A)
σ_p = conductivity of the pore fluid (3.5.3)

2.2—Definitions

ACI provides a comprehensive list of definitions through an online resource, "ACI Concrete Terminology," http://terminology.concrete.org.

CHAPTER 3—SUMMARY OF METHODS

Chapter 3 reviews the various nondestructive test (NDT) methods for evaluating concrete for characteristics other than strength. The underlying principles are discussed, the instrumentation is described, and the inherent advantages and limitations of each method are summarized. Where it is appropriate, examples of test data are provided. Table 3 summarizes the methods to be discussed. The first column lists the report section where the method is described, the second column provides a brief explanation of the underlying principles, and the third column gives typical applications.

Most NDT methods are indirect tests because the condition of the concrete is inferred from the measured response to some stimulus, such as impact or electromagnetic radiation. For favorable combinations of test method and site conditions, test results may be unambiguous and supplemental testing may be unnecessary. In other cases, the NDT results may be inconclusive and additional testing may be needed. Supplemental testing can be another NDT method, or often it may be an invasive method to allow direct observation of the internal condition. Invasive inspection can range from drilling small holes to removing test samples by coring or sawing. The combination of nondestructive and invasive inspection allows the reliability of the NDT method to be assessed for the specific project. Once the reliability of the

Table 3—Summary of nondestructive testing methods

Section no.	Method and principle	Applications
3.1	**Visual inspection**—Observe, classify, and document the appearance of distress on exposed surfaces of the structure.	Map patterns of distress such as cracking, spalling, scaling, erosion, or construction defects.
3.2.1	**Ultrasonic through transmission (pulse velocity)**—Measure the travel time of a pulse of ultrasonic waves over a known path length.	Determine the relative condition or uniformity of concrete based on measured pulse velocity.
3.2.2	**Ultrasonic-echo—**Transducer emits short pulse of ultrasonic waves, which is reflected by the opposite side of member or an internal defect; arrival of reflected pulse is recorded by an adjacent receiver (pitch-catch method), and round-trip travel time is determined.	Locate within concrete elements a variety of defects such as delaminations, voids, honeycombing, or measure element thickness.
3.2.3	**Impact-echo**—Receiver adjacent to impact point monitors arrival of stress wave as it undergoes multiple reflections between surface and opposite side of plate-like member or from internal defects. Frequency analysis permits determination of distance to reflector if wave speed is known.	Locate a variety of defects within concrete elements such as delaminations, voids, honeycombing, or measure element thickness.
3.2.4	**Spectral analysis of surface waves**—Impact is used to generate a surface wave and two receivers monitor the surface motion; signal analysis allows determination of wave speed as a function of wavelength; inversion process determines elastic constants of layers.	Determine the stiffness profile of a pavement system. Also used to determine depth of deteriorated concrete.
3.2.5 3.3.2	**Impulse-response**—Surface of element is struck with instrumented hammer and adjacent transducers measure dynamic response; signal analysis allows determining characteristics of tested element.	Locate anomalous regions in plate-like structures. Locate voids below slabs-on-ground. Locate cracks or constrictions (neck-in) in deep foundations. Provides information on the low-strain dynamic stiffness of the shaft/soil system.
3.3.1	**Sonic-echo**—Hammer impact on surface and a receiver monitors reflected stress wave. Time-domain analysis used to determine travel time.	Determine the length of deep foundations (piles and piers); determine the location of cracks or constrictions (neck-in).
3.3.2	**Impulse-response (mobility) method**—Surface of element is struck with instrumented hammer and adjacent transducers measure dynamic response; frequency domain signal analysis allows determining characteristics of tested element.	Determine the length of deep foundations (piles and piers); determine the location of cracks or constrictions (neck-in).
3.3.3	**Impedance logging**—Test is similar to sonic-echo or impulse-response, but the use of more complex signal analyses (time and frequency domains) allows reconstructing the approximate shape of the deep foundation.	Determine the approximate two-dimensional (2-D) shape of the deep foundation.
3.3.4	**Crosshole sonic logging (CSL)**—Analogous to the ultrasonic pulse velocity (UPV) test, but transducers are positioned within water-filled tubes cast into the deep foundation or holes drilled after construction.	Determine the location of low-quality concrete and defects along the length of the shaft and between transducers. With drilled holes permits direct determination of shaft length.
3.3.5	**Parallel seismic**—Receiver is placed in hole adjacent to the foundation. Foundation is struck with a hammer and signal from receiver is recorded. Test is repeated with receiver at increasing depth.	Determine the foundation depth and determine whether it is of uniform quality.
3.4.2	**Direct transmission radiometry for density**—Measure the intensity of high-energy electromagnetic radiation after passing through concrete.	Determine in-place density of fresh or hardened concrete. Locate reinforcing steel or voids.
3.4.3	**Backscatter radiometry for density**—Measure the intensity of high-energy electromagnetic radiation that is backscattered (reflected) by the near-surface region of a concrete member.	Determine in-place density of fresh or hardened concrete.
3.4.4	**Radiography**—The intensity of high-energy electromagnetic radiation, which passes through a member, is recorded on photographic film.	Locate reinforcing and prestressing steel, conduits, pipes, voids, and honeycombing.
3.4.5	**Gamma-gamma logging of deep foundations**—See direct transmission and backscatter radiometry. Radioactive source and detector are lowered into separate access tubes cast into deep foundation.	Locate regions of low density along length of foundation.
3.5.1	**Covermeters—**Sometimes known as a reinforcing bar locator, is a low-frequency alternating magnetic field applied on the surface of the structure; the presence of embedded reinforcement alters this field, and measurement of this change provides information on the reinforcement.	Locate embedded steel reinforcement, measure depth of cover, estimate diameter, and determine direction of reinforcement.
3.5.2	**Half-cell potential**—Measure the potential difference (voltage) between the steel reinforcement and a standard reference electrode; the measured voltage provides an indication of the likelihood that corrosion is occurring in the reinforcement.	Identify region or regions in a reinforced concrete structure where there is a high probability that corrosion is occurring at the time of the measurement.
3.5.3	**Concrete resistivity**—In four-electrode method, often called Wenner Array, measures the electric potential between two inner electrodes due to current between two outer electrodes. Calculate resistivity based on assumed model.	Used to supplement half-cell potential survey; regions of low resistivity may be associated with high corrosion rate of reinforcement if there is active corrosion. In the laboratory, method can be used to assess resistance to fluid transport of saturated specimens.

Table 3—Summary of nondestructive testing methods (cont.)

3.5.4	**Linear polarization resistance**—Apply small current and measure change in the potential difference between the reinforcement and a standard reference electrode; the measured current and voltage changes allow determination of the polarization resistance, which is related to the rate of corrosion.	Determine the instantaneous corrosion rate of the reinforcement located below the test point. By taking readings at key times during an annual cycle, one can approximate service life.
3.5.5	**Magnetic-flux leakage**—Strong magnetic field is applied to a reinforced concrete member. The field induces a magnetic flux in the reinforcement. If there is a fractured bar or wire, flux is disrupted and magnetic lines flow out of the concrete, which are detected by a magnetic field sensor. Presence of flux leakage is used as indicator of wire break.	Commonly used for pipeline inspection of welds. Has been adapted for detecting wire breaks in prestressed concrete members.
3.6	**Methods for measuring transport properties**—Measure the flow of a fluid (air or water) into concrete under prescribed test conditions; the flow rate depends on the transport properties of the concrete. Transport may be by permeation, absorption, diffusion, or their combination.	Compare alternative concrete mixtures. Primarily research tools, but have the potential to be used for assessing adequacy of curing process.
3.7	**Infrared thermography**—The presence of flaws within the concrete affects the heat conduction properties of the concrete and the presence of defects are indicated by differences in surface temperatures when the test object is exposed to correct ambient conditions. Under controlled, pulsed heating conditions, the evolution of the surface temperature distribution can be related to relative flaw depth.	Locate near-surface delaminations in pavements and bridge decks. Well-suited for detecting delaminations in fiber-reinforced polymer laminates used for strengthening concrete members. Also widely used for detecting moist insulation in buildings.
3.8	**Radar**—Analogous to the ultrasonic pitch-catch method except that electromagnetic waves are used instead of stress waves. Interface between materials with different dielectric properties results in reflection of a portion of incident electromagnetic pulse.	Locate metal embedments, voids beneath pavements, and regions of high moisture contents; determine thickness of members.

NDT method is established, a thorough inspection of the structure can be completed economically.

3.1—Visual inspection

3.1.1 *General*—Normally, a visual inspection is one of the first steps in the evaluation of a concrete structure (Perenchio 1989). Visual inspection performed by a qualified investigator can provide a wealth of information that may lead to positive identification of the cause of observed distress. Broad knowledge in structural engineering, concrete materials, deterioration mechanisms, and construction methods is needed to extract the most information from the visual inspection. ACI 201.1R, ACI 207.3R, ACI 224.1R, ACI 362.2R, and ACI 349.3R provide information for recognizing and classifying different types of damage and can help to identify the probable cause of the distress.

3.1.2 *Planning*—Before undertaking a detailed visual inspection, the investigator should develop and follow a preestablished plan to maximize the quality of the recorded data. A suitable approach typically involves the following activities:

a) Cursory walk-through inspection to become familiar with the structure

b) Gathering background documents and information on the design, construction, ambient conditions, and operation and maintenance of the structure

c) Planning the complete investigation

d) Selecting necessary tools and appropriate safety equipment; laying out a control grid on the structure to serve as a basis for recording observations

e) Undertaking the visual inspection

f) Performing necessary supplemental tests

ACI 207.3R, ACI 224.1R, ACI 349.3R, ACI 362.2R, and ACI 437R should be consulted for additional guidance on planning and carrying out the complete investigation.

3.1.3 *Supplemental tools*—Visual inspection is one of the most versatile and powerful of all the NDT methods; however, its effectiveness depends on the knowledge and experience of the investigator. It has the obvious limitation that only visible surfaces can be inspected. Internal defects go unnoticed and no quantitative information is obtained about the properties of the concrete. For these reasons, a visual inspection is usually supplemented by one or more of the other NDT methods discussed in this chapter. The inspector should consider other useful tools that can enhance the power of a visual inspection.

Optical magnification allows for a more detailed view of local areas of distress. Available instruments range from simple magnifying glasses to more expensive hand-held microscopes. Understanding the fundamental principles of optical magnification is helpful in selecting the correct tool. For example, the focal length decreases with increasing magnifying power, requiring the primary lens be placed closer to the surface being inspected. The field of view also decreases with increasing magnification, making it tedious to inspect a large area at high magnification. The depth of field is the maximum difference in elevation of points on a rough textured surface that are simultaneously in focus; this decreases with increasing magnification of the instrument. To assure that the hills and valleys are in focus simultaneously, the depth of field has to be greater than the elevation differences in the texture of the surface that is being viewed. The illumination required to see clearly increases with magnification level with artificial lighting necessary at high magnification.

A useful tool for crack inspection is a small hand-held magnifier with a built-in measuring scale on the lens closest to the surface being viewed (ACI 224.1R). With such a crack comparator, the width of surface cracks can be measured accurately.

A stereo microscope includes two viewing lenses that allow a three-dimensional observation of the surface. By calibrating the focus adjustment screw (change in height per screw revolution), the investigator can estimate the elevation

differences in surface features. This is done by first focusing on the lowest point within the field of view and determining how many turns of the screw it takes to bring the highest point into focus.

Fiberscopes and borescopes allow inspection of regions that are otherwise inaccessible to the naked eye. A fiberscope is composed of a bundle of optical fibers and a lens system; it allows viewing into cavities within a structure by means of small access holes. The fiberscope is designed so that some fibers transmit light to illuminate the cavity. The operator can rotate the viewing head to allow a wide viewing angle from a single access hole. A borescope, which is composed of a rigid tube with mirrors and lenses, is designed to view straight ahead or at right angles to the tube. The image is clearer using a borescope, whereas the fiberscope offers more flexibility in the field of view. The use of these scopes requires drilling small holes if other access channels are absent, and the holes should intercept the cavity to be inspected. Additional methods discussed in this chapter may be used to locate these cavities. Therefore, the fiberscope or borescope may be used to verify the results of other NDT methods without having to take cores. The locations of drilled access holes need to be chosen carefully to avoid drilling into utility conduits or reinforcing steel.

Flexibility of visual inspection was expanded by development of the small, inexpensive, digital video camera. These are used like borescopes with the added benefit of video output that can be displayed on a monitor and stored on the appropriate recording media. These cameras have various optical systems that come in a variety of sizes, resolutions, and focal lengths. Miniature versions attached to the ends of flexible shafts are available. These can be inserted into holes drilled into the structure for views of internal cavities. Alternatively, these small cameras can be mounted on robotic devices for inspections in pipes, or within areas that pose health or safety hazards.

3.1.4 *Reliability*—The Federal Highway Administration (FHWA) conducted a study to evaluate the reliability of visual inspection of bridges (Moore et al. 2001). Although there are differences in inspecting bridges compared with buildings, the study provides insight into the limitations of visual inspection. The study sought to evaluate the reliability of routine, in-depth bridge inspections; the influence of key factors on the results of visual inspections; and the differences in procedures and report formats for different states. The purpose of a bridge inspection is to assign a condition rating to the outcome, which numbers from 0 (failed condition) to 9 (excellent condition).

Routine inspections are regularly scheduled inspections consisting of observations, measurements, or both, that are required to determine the physical and functional condition of the bridge, to identify any changes from initial or previously recorded conditions, and to ensure that the structure continues to satisfy present service requirements (Moore et al. 2001). Results showed that 95 percent of ratings from routine inspections varied within two points of the average rating for a given bridge. Factors that appeared to correlate with the results included fear of traffic, visual acuity and color vision, formal inspection training, light intensity, and time constraints to complete the inspection. Interestingly, the following factors had minimal correlation to the bridge ratings assigned by the inspector: being a licensed engineer, general education level, and bridge inspection experience.

An in-depth inspection is a close-up, hands-on inspection of one or more members above or below the water level to identify any deficiency or deficiencies not readily detectable using routine inspection procedures (Moore et al. 2001). Results showed that in-depth inspections using visual inspection alone are not likely to detect the specific defects for which the inspection is prescribed, and they may not reveal deficiencies beyond those noted in routine inspections. Factors that appeared to relate to the results of an in-depth inspection include overall thoroughness with which the inspector completed the task, completion time, comfort with access equipment and heights, complexity of the structure and its accessibility, and flashlight use.

Based on the results of the study, authors of the FHWA report provided a set of recommendations that included the following (Moore et al. 2001):

a) Accuracy and reliability of in-depth inspections could be increased by increased training in the types of defects that should be identified and the best methods to use.

b) Factors that were found to correlate with inspection results should be considered in choosing and training inspectors.

c) Further study of the types of defects that could occur and are likely to be identified in concrete structures is warranted.

In summary, visual inspection is a powerful NDT method. Its effectiveness, however, is limited by the investigator's experience and knowledge. A broad knowledge of structural behavior, materials, and construction methods is desirable. Low-cost tools are available to extend the capabilities of visual inspection, which is typically only one aspect of the total evaluation plan. Visual inspections will often be supplemented by a series of other NDT methods or invasive procedures.

3.2—Stress-wave methods for structures

Several test methods based on stress-wave propagation can be used for nondestructive testing (NDT) of concrete structures. The ultrasonic through-transmission (pulse velocity) method can be used for locating abnormal regions in a member. The term "ultrasonic" refers to stress waves above the audible range, which is usually assumed to be above a frequency of 20 kHz.

The echo methods can be used for thickness measurements and flaw detection. The spectral analysis of surface waves (SASW) method can be used to determine the thickness and elastic moduli of layered pavement systems. The following subsections describe the principles and instrumentation for each method. Section 3.3 discusses stress-wave methods for integrity testing of deep foundations. Additional information is provided in Carino (2004a).

Stress waves occur when pressure or deformation is applied suddenly, such as by impact, to the surface of a solid. The disturbance propagates through the solid in a manner

analogous to how sound travels through air. The speed of stress-wave propagation in an elastic solid is a function of the Young's modulus of elasticity, Poisson's ratio, the density, and the geometry of the solid. This dependence between the properties of a solid and the resultant stress-wave propagation behavior permits inferences about the characteristics of the solid by monitoring the propagation of stress waves.

When pressure is applied suddenly at a point on the surface of a solid half-space, the disturbance propagates through the solid as three different waves: P-wave, S-wave, and R-wave. The P-wave and S-wave propagate into the solid along hemispherical wavefronts. The P-wave, also called the dilatational or compression (primary) wave, is associated with the propagation of normal stress and particle motion is parallel to the propagation direction. The S-wave, also called the shear or transverse wave, is associated with shear stress and particle motion is perpendicular to the propagation direction. In addition, an R-wave travels away from the disturbance along the surface. In an isotropic, elastic solid, the P-wave speed, C_p, is related to the Young's modulus of elasticity E; Poisson's ratio ν; and density ρ (Krautkrämer and Krautkrämer 1990)

$$C_p = \sqrt{\frac{E(1-\nu)}{\rho(1+\nu)(1-2\nu)}} \tag{3.2a}$$

The S-wave propagates at a slower speed, C_s, given by (Krautkrämer and Krautkrämer 1990)

$$C_s = \sqrt{\frac{G}{\rho}} \tag{3.2b}$$

where G is the shear modulus of elasticity.

A useful parameter is the ratio of S-wave speed to P-wave speed

$$\frac{C_s}{C_p} = \sqrt{\frac{1-2\nu}{2(1-\nu)}} \tag{3.2c}$$

For a Poisson's ratio ν of 0.2, which is typical of concrete, this ratio equals 0.61. The ratio of the R-wave speed, C_r, to the S-wave speed may be approximated by (Krautkrämer and Krautkrämer 1990)

$$\frac{C_r}{C_s} = \frac{0.87+1.12\nu}{1+\nu} \tag{3.2d}$$

For a Poisson's ratio ν between 0.15 and 0.25, the R-wave speed is from 90 to 92 percent of the S-wave speed.

Equation (3.2a) represents the P-wave speed in an infinite solid. In the case of bounded solids, wave speed is affected by the geometry of the solid. For wave propagation along the axis of slender bar, the wave speed of the dominant pulse is independent of Poisson's ratio and is given by

Table 3.2—*Z*-values for common materials

Material	Specific acoustic impedance, kg/(m²·s) (psi·s/ft)
Air	0.4 (1.7×10^{-5})
Water	1.5×10^6 (66)
Soil	0.3 to 4×10^6 (13 to 180)
Concrete	7 to 10×10^6 (310 to 440)
Limestone	7 to 19×10^6 (310 to 840)
Granite	15 to 17×10^6 (660 to 750)
Steel	47×10^6 (2100)

$$C_b = \sqrt{\frac{E}{\rho}} \tag{3.2e}$$

where C_b is the bar wave speed. For a Poisson's ratio between 0.15 and 0.25, the bar wave speed in a slender bar is 3 to 9 percent slower than the P-wave speed in a large solid.

When a stress wave traveling through Material 1 is incident on the interface between a dissimilar Material 2, a portion of the incident wave is reflected. The amplitude of the reflected wave is a function of the angle of incidence and is a maximum when this angle is 90 degrees (normal incidence). For normal incidence, the reflection coefficient R is given by

$$R = \frac{Z_2 - Z_1}{Z_2 + Z_1} \tag{3.2f}$$

where R is the ratio of sound pressure of the reflected wave to the sound pressure of the incident wave; Z_2 is the specific acoustic impedance of Material 2; and Z_1 is the specific acoustic impedance of Material 1.

The specific acoustic impedance is the product of the wave speed and density of the material. Table 3.2 shows approximate Z-values for some materials (Carino 2004a).

Thus, for a stress wave that encounters an air interface as it travels through concrete, the absolute value of the reflection coefficient is nearly 1.0, and there is almost total reflection at the interface. This is why NDT methods based on stress-wave propagation have proven to be successful for locating defects within concrete.

3.2.1 *Ultrasonic through transmission (pulse velocity) method*—One of the oldest NDT methods for concrete is based on measuring the travel time over a known path length of a pulse of ultrasonic compressional waves. The technique is known as ultrasonic through transmission or, more commonly, as the ultrasonic pulse velocity (UPV) method. Naik et al. (2004) provide a summary of this test method, and Tomsett (1980) reviewed the various applications of the technique.

The development of field instruments to measure the pulse velocity occurred nearly simultaneously in the late 1940s in Canada and England (Whitehurst 1967). In Canada, there was a need for an instrument that could measure the extent of cracking in dams (Leslie and Cheesman 1949). In the UK,

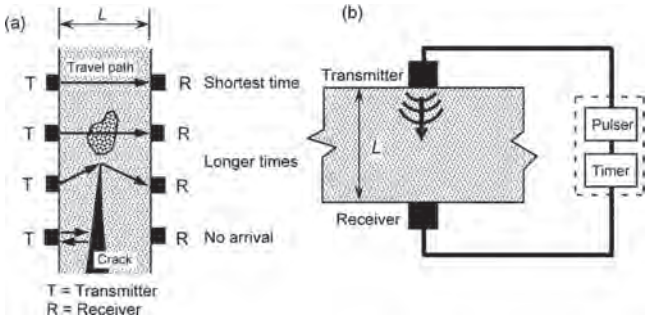

Fig. 3.2.1.1a—(a) Effects of defects on travel time of ultrasonic pulse; and (b) schematic of through-transmission test system.

the emphasis was on the development of an instrument to assess the quality of concrete pavements (Jones 1949).

3.2.1.1 *Principle*—The speed of propagation of stress waves depends on the density and the elastic constants of the solid. In a concrete member, variations in density can arise from non-uniform consolidation, and variations in elastic properties can occur due to variations in materials, mixture proportions, or curing. Thus, by determining the wave speed at different locations in a structure, it is possible to make inferences about the uniformity of the concrete. The compressional wave speed is determined by measuring the travel time of the stress pulse over a known distance.

The testing principle is illustrated in Fig. 3.2.1.1a(a), which depicts the paths of ultrasonic pulses as they travel from one side of a concrete member to the other. The top case represents the shortest direct path through sound concrete, which would result in the shortest travel time or the fastest apparent wave speed. The second case represents a path that passes through a portion of inferior concrete, and the third case shows a diffracted path around the edge of a large void or crack. In these latter cases, the travel time would be greater than the first case. The last case indicates a travel path that is interrupted by a void. This air interface results in total reflection of the stress waves with no arrival at the opposite side. The apparent wave speeds are determined by dividing the member thickness by the measured travel time. A comparison of the wave speeds at the different test points would indicate the areas of anomalies within the member. It might also be possible to use signal attenuation as an indicator of relative quality of concrete. This, however, requires special care to ensure consistent coupling of the transducers at all test points (Teodoru 1994).

An apparatus for through-transmission measurements has also been used on the same surface, as shown in Fig. 3.2.1.1b(a). This approach has been suggested for measuring the depth of a fire-damaged surface layer having a lower wave speed than the underlying sound concrete (Chung and Law 1985) and for measuring the depth of concrete damaged by freezing (Teodoru and Herf 1996). The test is carried out by measuring the travel time as a function of the separation, *X*, between transmitter and receiver. The method assumes that stress-wave arrival at the receiver occurs along two paths: Path 1, which is directly through the damaged concrete, and

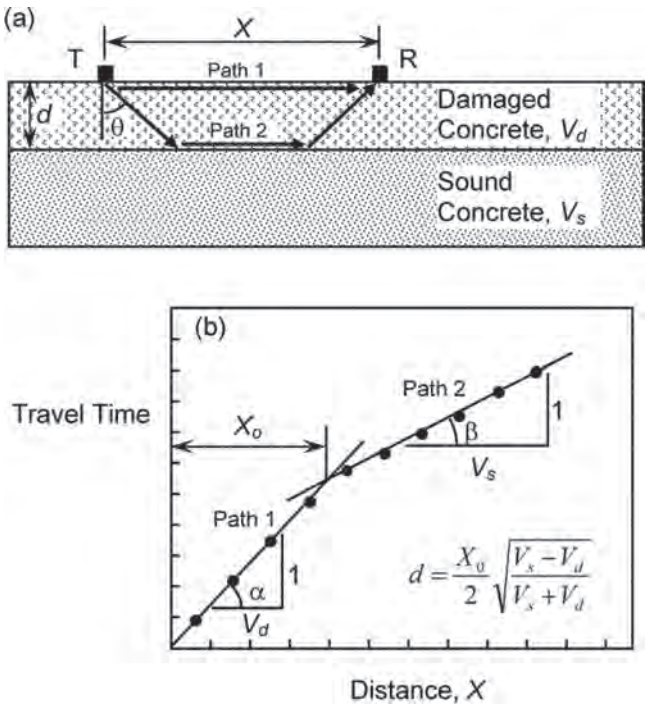

Fig. 3.2.1.1b—(a) Wave paths for ultrasonic testing on surface of concrete having damaged surface layer; and (b) travel time as a function of distance between transmitter and receiver.

Path 2, which is through the damaged and sound concrete. For small separation, the travel time is shorter for Path 1, and for large separation, the travel time is shorter for Path 2. By plotting the travel time as a function of the distance *X*, the presence of a damaged surface layer is indicated by a change in the slope of the data. The distance X_o, at which the travel times for the two paths are equal, is found from the intersection of the straight lines, as shown in Fig. 3.2.1.1b(b). The slopes of the two lines are reciprocals of the wave speeds in the damaged (V_d) and sound (V_s) concrete. The depth of the damaged layer is found using Eq. (3.2.1.1) (Chung and Law 1985).

$$d = \frac{X_o}{2}\sqrt{\frac{V_s - V_d}{V_s + V_d}} \qquad (3.2.1.1)$$

For the surface method, which relies on measuring the arrival time of low-amplitude waves, the user should understand the capabilities of the instrument to measure the correct arrival times. The user should also be familiar with the underlying theory of seismic refraction (Richart et al. 1970) that forms the basis of Eq. (3.2.1.1). The method is only applicable if the upper layer has a slower wave speed than the lower layer.

It is also possible to use multiple pulse velocity data to construct a two-dimensional (2-D) tomographic image of the interior of the concrete. This requires the ability to make multiple through-transmission measurements so that a chosen cross section is traversed by many direct ray paths. The cross section is modeled as a grid of elements whose

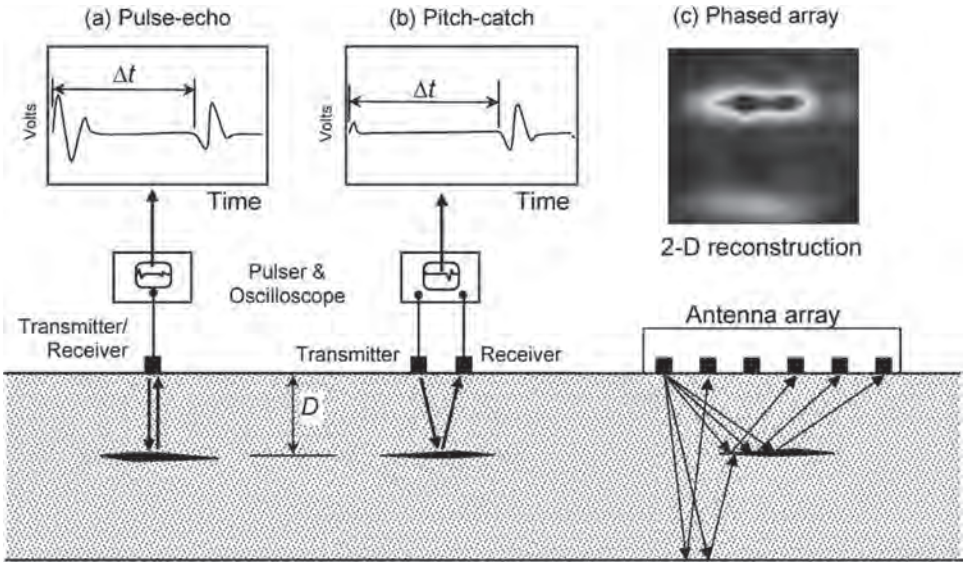

Fig. 3.2.2.1—Schematic of ultrasonic-echo methods: (a) pulse-echo method; (b) pitch-catch method; and (c) multiple pitch-catch using transducer array.

size depends on the number of measurements that are made. Based on the many calculated pulse velocities, computer software can be used to back-calculate a characteristic pulse velocity for each element. The result will be a 2-D image of the distribution of pulse velocity within the element cross section. Regions with abnormally low pulse velocity can then be identified as defects (Martin et al. 2001).

3.2.1.2 *Instrumentation*—The main components of modern devices for measuring the UPV are shown schematically in Fig. 3.2.1.1a(b). A transmitting transducer is positioned on one face of the member and a receiving transducer is positioned on the opposite face. The transducers contain piezoelectric ceramic elements. Piezoelectric materials change dimension when a voltage is applied to them, or they produce a voltage change when they are deformed. A pulser is used to apply a high voltage to the transmitting transducer (source), and the suddenly-applied voltage causes the transducer to vibrate at its natural frequency. The vibration of the transmitter produces the stress pulse that propagates into the member. At the same time that the voltage pulse is generated, an accurate electronic timer is turned on. When the pulse arrives at the receiver, the vibration is changed to a voltage signal that turns off the timer and the travel time is displayed. Requirements for a suitable pulse-velocity device are given in ASTM C597.

The transducers are coupled to the test surfaces using a viscous material, such as grease, or a nonstaining ultrasonic gel couplant if staining of the concrete is a problem. Transducers of various resonant frequencies have been used, with 50 kHz transducers being the most common. Generally, lower-frequency transducers are used for mass concrete (20 kHz) and higher-frequency transducers (>100 kHz) are used for thinner members, where accurate travel times have to be measured. In most applications, 50 kHz transducers are suitable.

3.2.2 *Ultrasonic-echo method*—Drawbacks of the through-transmission method include the need for access to both sides of the member and lack of information on the location (depth) of a detected anomaly. These limitations can be overcome by using the echo method, where testing is performed on one face of the member and the arrival time of a stress wave reflected from a defect is determined. This approach, which has been developed for testing metals, is known as the pulse-echo method. Since the 1960s, a number of different experimental ultrasonic-echo systems based on P-waves have been developed for concrete (Bradfield and Gatfield 1964; Howkins 1968). Successful applications have been limited mainly to measuring the thickness of and detecting flaws in thin slabs, pavements, and walls (Mailer 1972; Alexander and Thornton 1989). In the late 1990s, an ultrasonic-echo system based on S-waves and using multiple sensors was developed (Kozlov et al. 1997).

3.2.2.1 *Principle*—In the pulse-echo method, a stress pulse is introduced into an object at an accessible surface by a transmitter. The pulse propagates into the test object and is reflected by flaws or interfaces. The surface response caused by the arrival of reflected waves, or echoes, is monitored by the same transducer acting as a receiver. This technique is illustrated in Fig. 3.2.2.1(a). Due to technical problems in developing a suitable pulse-echo transducer for testing concrete, successful ultrasonic-echo methods have, in the past, used a separate receiving transducer located close to the transmitting transducer. This system, which is known as pitch-catch, is illustrated in Fig. 3.2.2.1(b). In early instruments, the receiver output was displayed on an oscilloscope as a time-domain waveform. The round-trip travel time of the pulse can be obtained from the waveform by determining the time from the start of the transmitted pulse to the reception of the echo. If the wave speed in the material is known, this travel time can be used to determine the depth of the reflecting interface. Pitch-catch systems developed in the 1990s use an array of transducers so that multiple pitch-catch measurements are made sequentially. The resulting

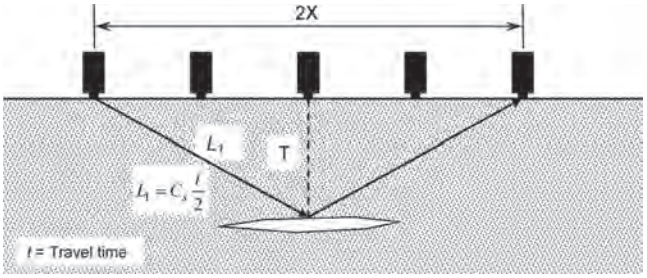

Fig. 3.2.2.2a—Principle of depth correction used in SAFT method.

travel time measurements are used to reconstruct an image of the reflecting interfaces. This type of system is illustrated in Fig. 3.2.2.1(c).

3.2.2.2 *Instrumentation*—The key components of a traditional pitch-catch ultrasonic-echo test system are the transmitting and receiving transducer(s), a pulser, and an oscilloscope or a computer for data acquisition and signal analysis. Transducers that transmit and receive short-duration, low-frequency (200 kHz) focused waves are needed for testing concrete. Note that a frequency of 200 kHz is considered low compared with the higher frequencies used in pulse-echo systems for testing metals, where frequencies in excess of 1 MHz are common.

In the early work, transmitting transducers were designed to have a focused P-wave field so that only the portion of the concrete directly below the transducers would be viewed. However, it was difficult to construct them and their dimensions often became large, making the transducers cumbersome and difficult to couple to the surface of the concrete (Mailer 1972). Although advances have resulted in improved transducers (Alexander and Thornton 1989), their penetration depths were limited to approximately 10 in. (250 mm).

A true pulse-echo system, where the source and receiver are one transducer, was developed and applied in the laboratory to concrete with small-sized aggregate (Hillger 1993). This system used a heavily damped 500 kHz transducer as both the source and receiver. A computer was used to process the data and display results using conventional techniques like ultrasonic testing of metals. One display method is the B-scan, where successive time-domain traces (obtained as the transducer is scanned over the test object) are oriented vertically and placed next to each other. The resulting plot is a cross-sectional view of the object showing the location of reflecting interfaces along the scan line. Because the system was cumbersome, requiring each transducer be cemented into place at each test point, a commercial system was never developed.

In the 1990s, dry point contact (DPC) transducers were developed that were capable of transmitting short pulses of low-frequency (less than 150 kHz) S-waves into concrete (Shevaldykin et al. 2003). The term "dry" means that no coupling fluid is necessary and the transducers are spring-loaded to ensure efficient coupling to irregular surfaces. These transducers are arranged in a 2-D array within a housing unit and operated on the pitch-catch principle as illustrated in Fig. 3.2.2.1(c). A computer software program is used to control the transducers so that they operate as transmitters and receivers in a predefined sequence. The result of a measurement is an array of round-trip travel times from transmitting to receiving transducers. Because of the inclined ray paths, as shown in Fig. 3.2.2.2a, the measured travel times between transducer pairs have to be corrected to obtain the correct depth of the reflecting interface. If the distance between the transmitter and receiver is 2*X*, the depth *T* of the reflecting interface is as follows

$$T = \sqrt{\left(C_s \frac{t}{2}\right)^2 - X^2} \qquad (3.2.2.2)$$

where C_s is the shear wave speed, and *t* is the travel time from transmitter to receiver.

A signal processing method known as the synthetic aperture focusing technique (SAFT) is used to reconstruct an internal image of the test object based on the corrected depths determined from Eq. (3.2.2.2) (Schickert et al. 2003; De La Haza et al. 2008). The reconstruction is done by representing the test object as a mesh of small elements, much like a finite-element mesh. From the known location of the transducer pairs and the corrected depths, the locations of reflectors are identified. The SAFT algorithm results in a constructed three-dimensional (3-D) image that can be viewed on any of three orthogonal image planes. The result is analogous to medical tomographic images that can be manipulated to look at different slices through the scanned object.

Figure 3.2.2.2b shows an example of a plain concrete block (Fig. 3.2.2.2b(a)) and an image (Fig. 3.2.2.2b(b)) that was obtained from a commercially available system. Figure 3.2.2.2b(a) shows a plain concrete masonry unit with a single 1.2 in. (30 mm) diameter hole at a depth of 5.1 in. (130 mm) and two 0.5 in. (13 mm) holes at depths of 2.2 in. (55 mm) and 6.3 in. (160 mm). In Fig. 3.2.2.2b(b), a 2-D image is shown that represents an end view of the block. The presence of the three holes is shown clearly. The back wall of the block is indicated as the light zone at the bottom of the image.

3.2.3 *Impact-echo method*—The idea of using an impact to generate a stress pulse is an old idea that has the advantage of eliminating the need for a bulky transmitting transducer and providing a stress pulse with greater penetration ability. However, the stress pulse generated by impact at a point is not focused like a pulse from an ultrasonic transducer. Instead, waves propagate into a test object in all directions, and reflections may arrive from many directions. Since the early 1970s, impact methods, usually called seismic-echo or sonic-echo methods, have been widely used for evaluation of concrete piles and drilled shaft foundations (Steinbach and Vey 1975). These foundation NDT methods are discussed in 3.3.1. Beginning in the mid-1980s, the impact-echo technique was developed for testing concrete structural members (Sansalone and Carino 1986; Sansalone 1997). Applications of the impact-echo technique include determining the thickness of and detecting flaws in plate-like structural members such as slabs and bridge decks with or without overlays;

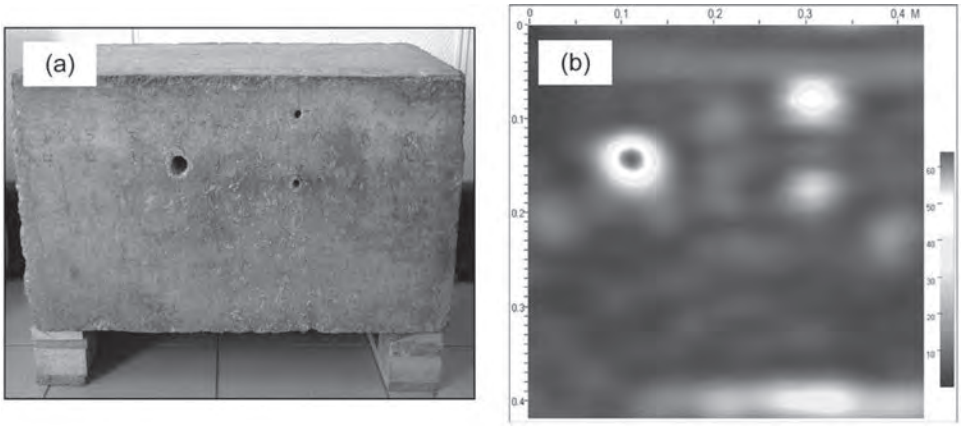

Fig. 3.2.2.2b—(a) Concrete block with three holes; (b) and elevation view based of SAFT reconstruction using multiple pitch-catch measurements (figure courtesy of Germann Instruments).

detecting flaws in beams, columns, and hollow cylindrical structural members; assessing the quality of bond in overlays; measuring crack depth; and voiding detection in grouted ducts of post tensioned bridge beams (Sansalone and Streett 1997; Sansalone and Carino 1988, 1989a,b; Lin and Sansalone 1992a,b,c; Cheng and Sansalone 1993; Lin and Sansalone 1993, 1994a,b, 1996; Lin and Su 1996; Abraham et al. 2002; Colla 2002; Muldoon et al. 2007). The use of the impact-echo method for determination of the thickness of concrete plate elements was standardized in ASTM C1383.

3.2.3.1 *Principle*—The principle of the impact-echo technique is illustrated in Fig. 3.2.3.1(a). A transient stress pulse is introduced into a test object by mechanical impact on the surface. The P- and S-waves produced by the stress pulse propagate into the object along hemispherical wavefronts. In addition, a surface wave travels along the surface away from the impact point. The waves are reflected by internal interfaces or external boundaries. The arrival of these reflected waves, or echoes, at the surface where the impact was generated produces displacements that are measured by a receiving transducer and recorded using a data-acquisition system. Interpretation of waveforms in the time domain has been successful in seismic-echo applications involving long, slender structural members such as piles and drilled shafts (Steinbach and Vey 1975; Olson and Wright 1990). In such cases, there is sufficient time between the generation of the stress pulse and the reception of the wave reflected from the bottom surface or from an inclusion or other flaw, so that the arrival time of the reflected wave is generally easy to determine, even if long-duration impacts produced by hammers are used.

Although for relatively thin structural members, such as slabs and walls, time-domain analysis is feasible if short-duration impacts are used, it is time consuming and can be difficult depending on the geometry of the structure (Sansalone and Carino 1986). The preferred approach, which is much quicker and simpler, is frequency analysis of displacement waveforms (Carino et al. 1986). The underlying principle of frequency analysis is that the waves generated by the impact undergo multiple reflections within the element and set up a resonant thickness mode vibration (Gibson and Popovics 2005). The frequency of this resonant vibration depends on the wave speed and the distance between the test surface and the reflecting interface or back wall of the element. For the case of reflections in a plate-like structure, this frequency is called thickness frequency. The frequency varies with the inverse of member thickness.

In frequency analysis, the time-domain signal is transformed into the frequency domain using the fast Fourier transform (FFT) technique. The result is an amplitude spectrum that indicates the amplitude of the various frequency components in the waveforms. The frequency corresponding to the setup resonance vibration—that is, the thickness frequency—is indicated by a peak in the amplitude spectrum. For a plate-like structure, the approximate relationship between the distance D to the reflecting interface, the P-wave speed C_p, and the thickness frequency f is

$$D = \frac{C_p}{2f} \tag{3.2.3.1}$$

For accurate assessment of plate thickness, the P-wave speed in Eq. (3.2.3.1) should be multiplied by a factor that ranges from 0.96 to 0.94, depending on material's Poisson's ratio (Gibson and Popovics 2005). In ASTM C1383, the P-wave speed is multiplied by 0.96.

As an example, Fig. 3.2.3.1(b) shows the amplitude spectrum obtained from an impact-echo test of a 20 in. (0.5 m) thick concrete slab. The peak at 3.42 kHz corresponds to the thickness frequency of the solid slab and a velocity of 11,200 ft/s (3420 m/s) is calculated. Figure 3.2.3.1(c) shows the amplitude spectrum for a test over a void within the same slab. The peak has shifted to a frequency of 7.32 kHz, indicating that the reflections are occurring from an interface within the slab. The ratio 3.42 kHz/7.32 kHz = 0.46 indicates that the interface is at approximately the middle of the slab with a calculated depth of 9 in. (0.23 m).

In using the impact-echo method to determine the locations of flaws within a slab or other plate-like structure,

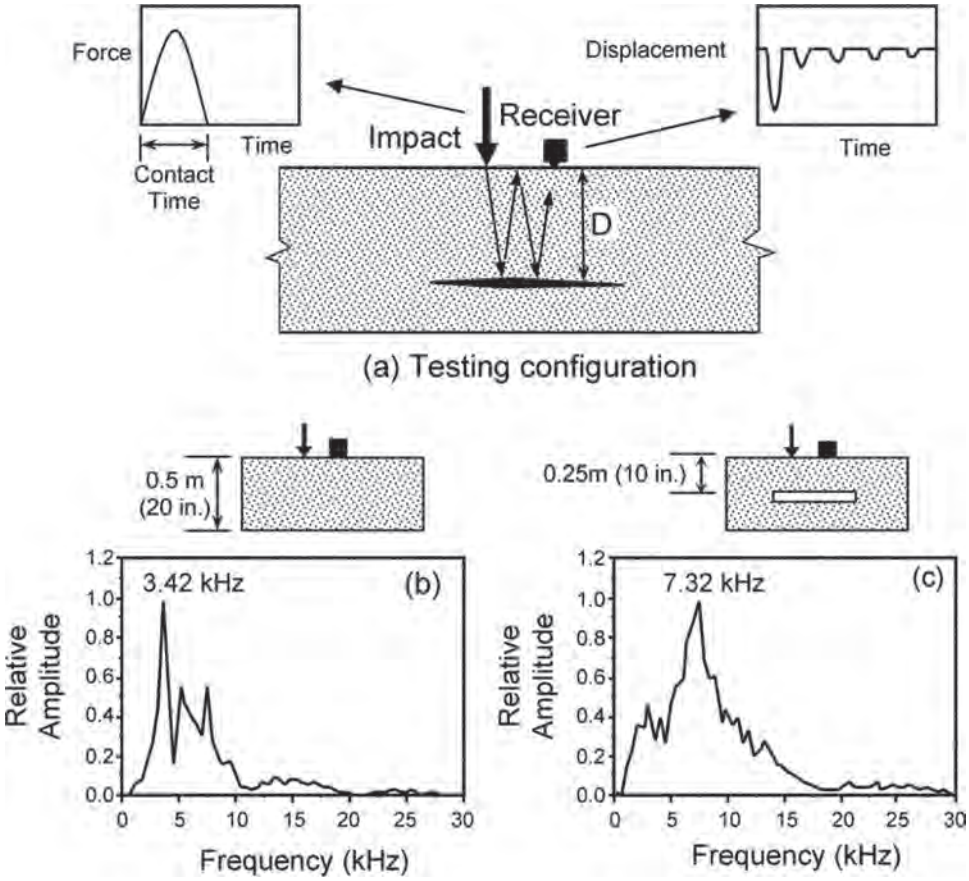

Fig. 3.2.3.1—(a) Schematic of impact-echo method; (b) amplitude spectrum for test of solid slab; and (c) amplitude spectrum for test over void in slab.

tests can be performed at regularly spaced points along lines marked on the surface. Spectra obtained from such a series of tests can be analyzed with the aid of computer software that can identify those test points corresponding to the presence of flaws and can plot a cross-sectional view along the test line (Pratt and Sansalone 1992).

Frequency analysis of signals obtained from impact-echo tests on bar-like structural elements, such as reinforced concrete beams and columns, bridge piers, and similar members, is more complicated than the case of slab-like structural members. The presence of the side boundaries gives rise to transverse modes of vibration of the cross section (Sansalone and Streett 1997). Thus, before attempting to interpret test results, the characteristic frequencies associated with the transverse modes of vibration of a solid structural member have to be determined. These frequencies depend on the shape and dimensions of the cross section. It has been shown that the presence of a flaw disrupts these modes, making it possible to determine that a flaw exists (Lin and Sansalone 1992a,b,c).

3.2.3.2 *Instrumentation*—An impact-echo test system, in accordance with ASTM C1383, is composed of three components: an impact source; a receiving transducer; and a data-acquisition system that is used to capture the output of the transducer, store the digitized waveforms, and perform signal analysis. A suitable impact-echo test system can be assembled from off-the-shelf components. Several field systems (hardware and analysis software) are commercially available.

The selection of the impact source is a critical aspect of a successful impact-echo test system. The impact duration determines the frequency content of the stress pulse generated by the impact and determines the minimum flaw depth that can be determined. As the impact duration is shortened, higher-frequency components are generated. In evaluation of piles, hammers are used that produce energetic impacts with long contact times (greater than 1 ms) suitable for testing long, slender structural members. Impact sources with shorter-duration impacts (20 to 80 μs), such as a spherical impactors, have been used for detecting flaws within structural members less than 40 in. (1 m) thick.

The impact duration, called the contact time, can be estimated from the width of the surface wave signal on the time-domain plot. The contact time of the impact used in the test influences several additional factors that determine the minimum depth and lateral dimension of the flaw that can be detected. These factors are as follows:

a) When spherical impactors are used, the contact time t_c for an elastic impact, assuming no local crushing of the concrete, is approximately a linear function of the ball diameter $t_c \approx 4.3D$ (μs units), where D is the impactor diameter, in millimeters.

b) The maximum useable frequency contained in the impact is approximately the inverse of the contact time ($f_{max} \approx 1/t_c$).

Table 3.2.3.2—Minimum depth and lateral dimension of flaw for detection by impact-echo using impactors of various diameters (C_p = 15,750 ft/s [4000 m/s])

Sphere diameter, in. (mm)	Contact time t_c, μs	Maximum useful frequency = $1/t_c$, kHz	Minimum depth of flaw that can be detected, in. (mm)	Minimum lateral dimension of flaw that can be detected, in. (mm)
0.20 (5)	22	47	1.69 (43)	3.39 (86)
0.25 (6.5)	28	36	2.20 (56)	4.41 (112)
0.31 (8)	34	29	2.72 (69)	5.43 (138)
0.37 (9.5)	41	24	3.22 (82)	6.42 (163)
0.43 (11)	47	21	3.74 (95)	7.44 (189)
0.5 (12.5)	54	19	4.25 (108)	8.46 (215)

c) Using Eq. (3.2.3.1), by replacing f with $1/t_c$, $D_{min} = C_p t_c/2$, which gives the smallest flaw depth, or plate thickness, that can be measured for a given wave speed and impact duration. This equates to half the wavelength (λ/2) associated with the resonant thickness frequency (Sansalone and Streett 1997; Martin and Forde 1995; Martin et al. 1998).

d) The minimum lateral dimension of a flaw that can be detected, regardless of depth, equals the wavelength associated with the maximum useable frequency ($\lambda = C_p/f = C_p t_c$) (Sansalone and Streett 1997).

e) The minimum lateral dimension of a flaw that can be detected is approximately 1/4 of its depth (Sansalone and Streett 1997).

Thus, the minimum lateral dimension of flaw that can be detected is affected both by the contact time and flaw depth (Sansalone and Streett 1997).

Assuming a P-wave speed through concrete of 15,750 ft/s (4000 m/s), Table 3.2.3.2 gives the minimum depth and lateral dimension of a flaw that can be detected for typical sizes of spherical impactors. The least lateral dimension assumes that this is greater than one-quarter of the flaw depth. The values in Table 3.2.3.2 are based on a maximum useful frequency equal to the inverse of the contact time. Sansalone and Streett (1997), however, suggest a maximum useable frequency of 1.25 times this value. The lower maximum frequency recommended herein is believed to be appropriate to provide a more conservative estimate of detectable flaw depth or size, which may account for some inelastic behavior during impact.

New methods of analysis for evaluating the condition of grouted tendon ducts that increase the usefulness of the impact-echo method have been developed:

a) It has been found that if the contact time is too long and does not contain useable frequencies greater than the resonant frequency corresponding to the depth of the void, the presence of the void results in a lower thickness frequency for the solid plate. The presence of an internal duct defect lowers the apparent stiffness of the material through the thickness, giving rise to a lower thickness resonance frequency, which would manifest itself as an apparent increase in the depth of the back wall of the structure. This frequency shift can often be used as an indication of a void and the test should be repeated using a smaller contact time (smaller impactor) (Sansalone and Streett 1997).

b) Presentation of impact-echo amplitude spectra in the form of B-scans (or frequency profiles), which makes it easier to identify changes in the frequency response corresponding to the back wall of the element due to the presence of voids in ducts (Abraham et al. 2002; Colla 2002).

c) Application of the stack imaging technique based on the impact-echo (SIBIE) (Ohtsu and Watanabe 2002; Muldoon et al. 2007). The SIBIE technique enhances the identification of internal reflectors, such as voided tendon ducts, using an impact-echo time signal obtained from a single test location. The impact duration should be relatively short to generate the needed resolution within the time signal; the impact from an aluminum bullet is used as the source of wave energy (Ohtsu and Watanabe 2002). In the analysis, the known cross section of a tested member is divided into square elements, and the travel distance from the impactor to the receiver through the center of each element is calculated. Spectral amplitudes corresponding to virtual resonant frequencies (Eq. (3.2.2.2)) are summarized at each element.

Thus, reflection intensity is estimated as a stack image at each element, which results in a contour map of the reflection intensity across the cross section of the tested member.

In evaluation of piles, geophones (velocity transducers) or accelerometers have been used as the receiving transducer. For impact-echo testing of slabs, walls, beams, and columns, a broad-band conically-tipped piezoelectric transducer (Proctor 1982) that responds to surface displacement has been used as the receiver (Sansalone and Carino 1986). Small accelerometers have also been used as the receiver. In this case, additional signal processing is carried out in the frequency domain to obtain the appropriate amplitude spectrum (Olson and Wright 1990). Such accelerometers should have resonant frequencies well above the anticipated thickness frequencies to be measured.

ASTM adopted the C1383 test method on the use of the impact-echo method to measure the thickness of plate-like concrete members. ASTM C1383 defines a plate as a structure or portion of a structure in which the lateral dimensions are at least six times the thickness. The test method includes two procedures. Procedure A measures the P-wave speed in the concrete, and Procedure B determines the thickness frequency using the impact-echo method. Thickness is calculated from the wave speed and thickness frequency. P-wave speed may be determined by measuring the P-wave speed at the surface using two transducers (Sansalone et al. 1997). Alternately, the P-wave speed may be determined by measuring the thickness frequency at a point and then drilling a hole to measure the actual thickness. Limited comparisons with the length of drilled cores demonstrated

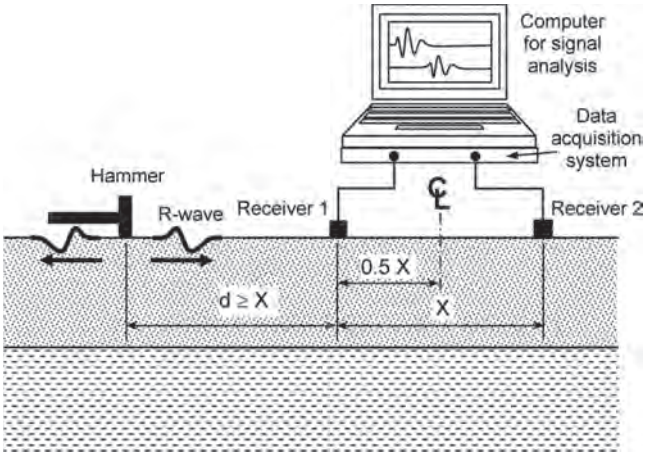

Fig. 3.2.4.1a—Schematic of spectral analysis of surface wave (SASW) method.

that the impact-echo results were within 3 percent of the core lengths (Sansalone and Streett 1997).

3.2.4 *Spectral analysis of surface waves (SASW) method*—In the late 1950s and early 1960s, Jones reported on the use of surface waves to determine the thickness and elastic stiffness of pavement slabs and of the underlying layers (Jones 1955, 1962). The method involved determining the relationship between the wavelength and velocity of surface vibrations as the vibration frequency was varied. Apart from the studies reported by Jones and work in France during the 1960s and 1970s, there seems to have been little additional use of this technique for testing concrete pavements. In the early 1980s, however, researchers at The University of Texas at Austin began studies of a surface wave technique that involved an impactor or vibrator that excited a range of frequencies. Digital signal processing, SASW, was used to develop the relationship between wavelength and velocity (Heisey et al. 1982; Nazarian et al. 1983). The SASW method has been used successfully to determine the elastic modulus profiles of soil sites, asphalt and concrete pavement systems, and concrete structural members. The method has been extended to the measurement of changes in the elastic properties of concrete slabs during curing and assessment of damage (Bay and Stokoe 1990; Kalinski 1997).

3.2.4.1 *Principle*—The general test configuration is illustrated in Fig. 3.2.4.1a (Nazarian and Stokoe 1986a). An impact is used to generate a surface or R-wave. Two receivers are used to monitor the motion as the R-wave propagates along the surface. The received signals are processed and a subsequent calculation scheme is used to infer the stiffness of the underlying layers.

Just as the stress pulse from impact contains a range of frequency components, the R-wave also contains a range of components of different frequencies or wavelengths. The product of frequency and wavelength equals wave speed. This range depends on the contact time of the impact; a shorter contact time results in a broader range. The longer-wavelength or lower-frequency components penetrate more deeply, which is the key to using the R-wave to gain information about the properties of the underlying layers (Rix and Stokoe 1989). In a layered system, the propagation speed of these different components is affected by the wave speed in those layers through which the components propagate. A layered system is a dispersive medium for R-waves, which means that different frequency components of the R-wave propagate with different speeds, which are called phase velocities.

Phase velocities are calculated by determining the time it takes for each frequency (or wavelength) component to travel between the two receivers. These travel times are determined from the phase difference of the frequency components arriving at the receivers (Nazarian and Stokoe 1986b). The phase differences are obtained by computing the cross-power spectrum of the signals recorded by the two receivers. The phase portion of the cross-power spectrum gives phase differences in degrees as a function of frequency. The phase velocities are determined as

$$C_{R(f)} = X\frac{360}{\phi_f}f \qquad (3.2.4.1a)$$

where $C_{R(f)}$ is the surface wave speed of component with frequency f; X is the distance between receivers (refer to Fig. 3.2.4.1a); and ϕ_f is the phase angle of component with frequency f.

The wavelength λ_f corresponding to a component frequency is calculated using the equation

$$\lambda_f = X\frac{360}{\phi_f} \qquad (3.2.4.1b)$$

By repeating the calculations in Eq. (3.2.4.1a) and (3.2.4.1b) for each component frequency, a plot of phase velocity versus wavelength is obtained. Such a plot is called a dispersion curve. Figure 3.2.4.1b(a) shows an example of a dispersion curve obtained by Nazarian and Stokoe (1986a) from tests on a concrete pavement. The short-wavelength components have higher speeds because they correspond to components traveling through the concrete slab.

A process called inversion is used to obtain the approximate stiffness profile at the test site from the experimental dispersion curve (Nazarian and Stokoe 1986b; Nazarian and Desai 1993; Yuan and Nazarian 1993). Although this process is called inversion, the technique actually uses forward modeling, with trial and error, until there is agreement between the measured and computed dispersion curves. The test site is modeled as layers of varying thickness. Each layer is assigned a density and elastic constants. Using this information, the solution for surface wave propagation in a layered system is obtained and a theoretical dispersion curve is calculated for the assumed layered system. The theoretical curve is compared with the experimental dispersion curve. If the curves match, the problem is solved and the assumed stiffness profile is correct. If there are significant discrepancies, the assumed layered system is changed or refined and a new theoretical curve is calculated. This process continues

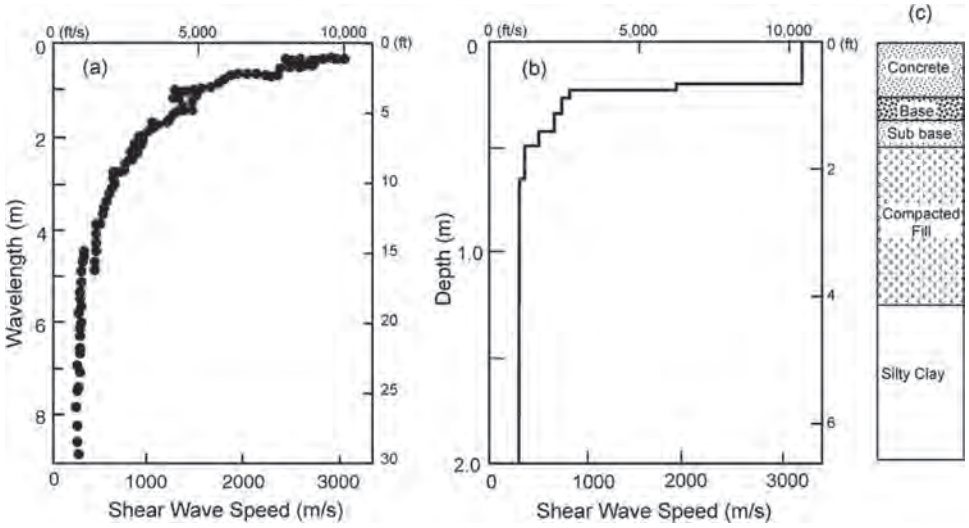

Fig. 3.2.4.1b—(a) Dispersion curve obtained from SASW testing of concrete pavement; (b) S-wave speed obtained from inversion of experimental dispersion curve; and (c) soil profile based on boring (adapted from Nazarian and Stokoe [1986a]).

until there is a satisfactory agreement between the theoretical and experimental curves. Figure 3.2.4.1b(b) shows the wave speed versus depth profile that corresponds to the dispersion curve, whereas the soil profile described in Fig. 3.2.4.1b(c) shows the actual conditions.

3.2.4.2 *Instrumentation*—There are three components to an SASW test system (Fig. 3.2.4.1a)

1. Although the energy source is usually a hammer, it could also be a vibrator with variable frequency excitation
2. Two receivers that are geophones (velocity transducers) or accelerometers
3. A two-channel data acquisition system and a computer for recording and processing the waveforms

The required characteristics of the impact source depend on the elastic modulus of the layers, the distances between the two receivers, and the depth to be investigated (Nazarian et al. 1983). When investigating concrete pavements and structural members, the receivers are located relatively close together. In this case, a small hammer, or even smaller impactor or vibrator, is required so that a short-duration pulse is produced with sufficient energy at frequencies up to approximately 50 to 100 kHz. As the depth to be investigated increases, the distance between receivers is increased, and an impact that generates a pulse with greater energy at lower frequencies is required. Thus, heavier hammers, such as a sledge hammer, are used.

The two receiving transducers measure vertical surface velocity or acceleration. The selection of transducer type depends in part on the test site (Nazarian and Stokoe 1986a). For tests where deep layers are to be investigated and a larger receiver spacing is required, geophones are generally used because of their superior low-frequency sensitivity. For tests of concrete pavements, the receivers should provide accurate measurements at higher frequencies. Thus, for pavements, a combination of geophones and accelerometers is often used. For concrete structural members, small accelerometers and small impactors or high-frequency vibrators are typically used (Bay and Stokoe 1990).

The receivers are first located close together and the spacing is increased by a factor of two for subsequent tests. As a check on the measured phase information for each receiver spacing, a second series of tests is carried out by reversing the position of the source. Typically, five receiver spacings are used at each test site. For tests of concrete pavements, the closest spacing is usually approximately 6 in. (0.15 m) (Nazarian and Stokoe 1986b).

3.2.5 *Impulse response method*—This method was initially developed in the 1970s for testing deep foundations (refer to 3.3). Its application to general concrete structures occurred in the 1990s. The impulse response method uses a low-strain impact to send a stress wave through the tested element. The time history of impact force is measured by an instrumented hammer. The maximum compressive stress at the impact point in concrete is related directly to the elastic properties of the impactor tip. Typically a 3 lb (1.5 kg) hammer with a plastic tip is used. The impact duration is much longer than in the impact-echo method. The long-duration impact in the impulse-response method means that the structural element responds to the impact in a bending vibration mode over a much lower frequency range (0 to 1 kHz for plate structures), as opposed to a higher frequency thickness mode of the impact-echo test. Response may be measured with an appropriate geophone with a linear response from a very low frequency (approximately 20 Hz) up to 1 kHz. Research for the impulse response method applied to structural concrete began in the mid-1980s (Pederson and Senkowski 1986; Davis and Hertlein 1987). In 2010, ASTM adopted a standard practice on using impulse response to evaluate the condition of concrete plates (ASTM C1740). Applications of the impulse response method include:

a) Voiding beneath concrete pavements, as well as spillway and floor slabs (Davis and Hertlein 1987)

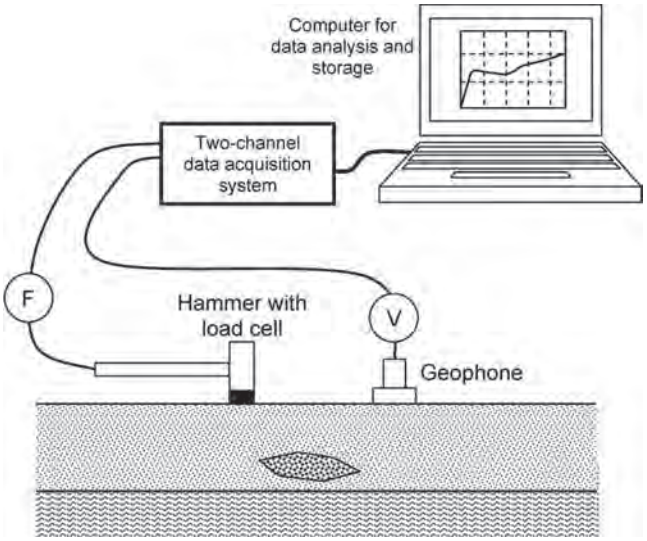

Fig. 3.2.5.1a—Schematic of impulse response method applied to plate-like structures.

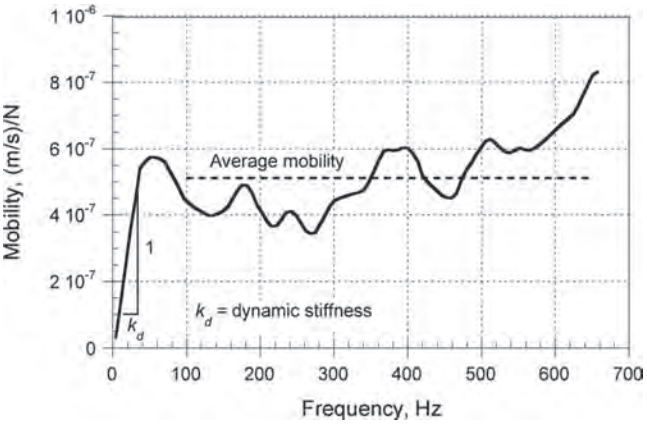

Fig. 3.2.5.1b—Impulse response mobility-frequency plot for a sound response.

b) Delamination of concrete around steel reinforcement in slabs

c) Walls and large structures such as dams, chimney stacks, and silos (Davis and Hertlein 1995)

d) Location of low-density concrete (honeycombing) and cracking in concrete elements (Davis and Hertlein 1995; Davis et al. 1997)

e) Depth of alkali-silica reaction attack in drilled shafts used as pylon foundations (Davis and Kennedy 1998)

f) Debonding of asphalt and concrete overlays to concrete substrates (Davis et al. 1996)

g) The degree of stress transfer through load-transfer systems across joints in concrete slabs (Davis and Hertlein 1987)

Davis (2002) presents a review of these applications.

3.2.5.1 *Principle*—The general test configuration is illustrated in Fig. 3.2.5.1a. A transient stress pulse is introduced into the test element by mechanical impact on the surface. The resultant bending behavior of the element is analyzed to characterize the integrity of the element. Both the time records for the hammer force and the geophone velocity response are processed in the field computer using the fast Fourier transform (FFT) algorithm. The resulting velocity spectrum is divided by the force spectrum to obtain a transfer function called the mobility of the element under test. The plot of mobility (vertical axis) versus frequency (horizontal axis) over the range of 0 to 1 kHz is called the mobility plot. Figure 3.2.5.1b is an example of a mobility plot, where the vertical axis is in units of speed per unit of force.

The mobility plot contains information on the condition and the integrity of the concrete in the tested elements, obtained from the following measured parameters.

3.2.5.1.1 *Dynamic stiffness*—The slope of the portion of the mobility plot below 0.1 kHz defines the compliance or flexibility of the area around the test point for a normalized force input. The inverse of the compliance is the dynamic stiffness of the structural element at the test point. The dynamic stiffness of a plate-like element depends on the thickness of the plate, the density and elastic modulus of the material, and the support conditions.

3.2.5.1.2 *Mobility and damping*—The test element's response to the impact-generated elastic wave will be damped by the element's intrinsic rigidity (body damping). For example, the mean mobility value over 0.1 to 1 kHz is directly related to the density and the thickness of a plate element. A reduction in plate thickness corresponds to an increase in mean mobility. As an example, when total debonding of an upper layer is present, a higher mean mobility reflects the thickness of the upper debonded layer (the slab becomes more mobile). Also, any cracking or honeycombing in the concrete will reduce the body damping and stability of the mobility plots over the tested frequency range. As a result, the mobility plot will display an increasing mobility with frequency above approximately 0.1 kHz.

3.2.5.1.3 *Peak/mean mobility ratio*—When debonding or delamination is present within a structural element, or when there is loss of support beneath a concrete slab-on-ground, the response behavior of the uppermost layer controls the impulse response test result. In addition to the increase in mean mobility between 0.1 and 1 kHz, the dynamic stiffness decreases greatly. The peak mobility below 0.1 kHz becomes appreciably higher than the mean mobility from 0.1 to 1 kHz. The result is a mobility plot with a high amplitude peak at low frequency. The ratio of this peak-to-mean mobility is an indicator of the presence and degree of either debonding within the element or voiding or loss of support beneath a slab-on-ground.

Test points are usually laid out on the test element surface in a grid pattern spacing (20 to 40 in. [0.5 to 1 m]), and the parameters of average mobility, stiffness, mobility slope, and peak-to-mean mobility ratio for each test point are measured. The results for each parameter are presented in the form of a contour plot representing a plan of the area tested. From this contour plot, comparative results enable overall assessments to be made. Figure 3.2.5.1.3 shows an example of a contour plot of average mobility obtained by testing a floor (slab-on-ground). The darker shading represents higher mobility. It is seen that higher mobility was obtained at the corners of the slab. This could be an indication that the slab has lifted off

the ground at the corners. There also appears to be a location of high mobility at grid point C7-R9 that would merit further investigation.

The results from impulse response tests, such as the dynamic stiffness or average mobility, cannot be readily predicted from engineering mechanics theory due to the potential variation in support and subgrade conditions. Therefore, the evaluation of impulse-response tests is typically performed in a comparative manner, with the change or variation in results between test points used to identify anomalous conditions.

3.2.5.2 *Instrumentation*—An impulse response test system is composed of three main components:

1. An impact source

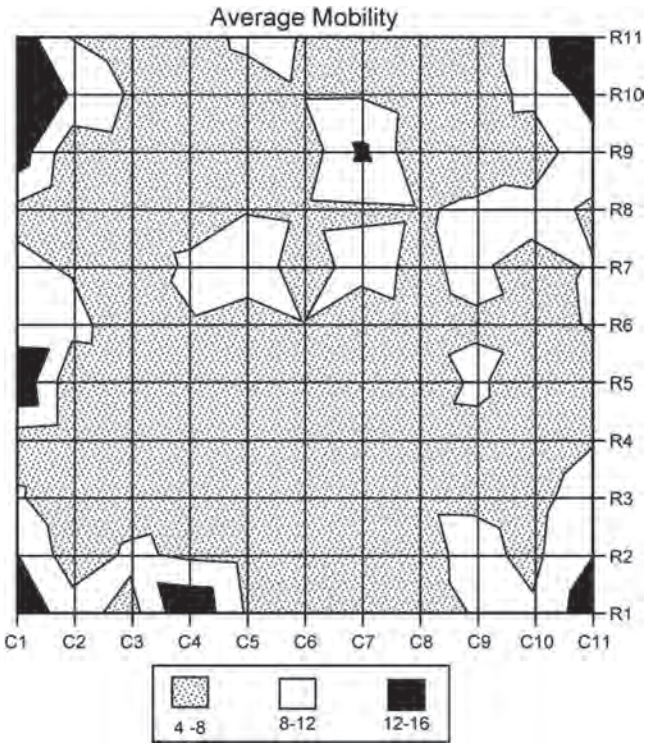

Fig. 3.2.5.1.3—Contour plot of average mobility values from a concrete floor slab.

2. A receiving transducer and twin-channel data acquisition system that are used to capture the output signals from the impactor and the receiving transducer, store the digitized waveforms, and perform signal analysis

3. An impulse response system that can be assembled from off-the-shelf components

In 2002, a complete field system for structure testing, including hardware and analysis software, became commercially available.

The impactor is normally a 3 lb (1.5 kg) sledgehammer equipped with a load cell to measure the force-time trace for each hammer blow. The 2 in. (51 mm) diameter hammer tip is composed of hard neoprene to obtain a useful force spectrum over a minimum range of 0 to 1.5 kHz. Larger or smaller hammers may produce clearer results, depending on slab thickness and support conditions, but the useful frequency range changes as a function of hammer mass. The receiving transducer is usually a velocity transducer or geophone mounted in a ruggedized plastic case. The response from a typical geophone is direction sensitive. Therefore, different geophone types are used to monitor displacement in different directions (that is, horizontal geophone, vertical geophone). Curved surfaces, such as tunnel linings, can be tested using triaxial geophones. The advantages of geophones over accelerometers are the direct measurement of velocity and their stability at low frequencies to 5 Hz.

3.2.6 *Advantages and limitations*—Each of the stress-wave propagation methods has distinct advantages and limitations summarized in Table 3.2.6. The UPV and impact echo methods have been standardized by ASTM with a variety of commercial devices available. The SASW method suffers from the complexity of the signal processing, but there have been efforts to automate this signal processing (Nazarian and Desai 1993).

3.3—Low strain stress-wave methods for deep foundations

During the 1930s, viable stress-wave methods for evaluation of deep foundations originated in the pile-driving industry. They were initially developed as a means of predicting pile capacity from the measured resistance of the pile to each driving hammer impact. When electronic

Table 3.2.6—Advantages and limitations of stress-wave methods for structures

Method	Advantages	Limitations
Ultrasonic through or direct transmission (pulse velocity) (ASTM C597)	Portable equipment is available; relatively easy to use.	Requires access to two sides of members; does not provide information on depth of defect.
Ultrasonic-echo	Access to only one face is needed; provides information on depth of defect. Method based on S-wave point transducers and SAFT permit construction of 3-D tomographic images.	Applicable to limited member thickness; experienced operator is required.
Impact-echo (ASTM C1383 for plate thickness)	Access to only one face is needed; equipment is commercially available; capable of locating a variety of defects; does not require coupling materials.	Experienced operator is required; current instrumentation limited to testing members 40 in. (1 m) thick.
Spectral analysis of surface waves	Capable of determining the elastic properties of layered systems, such as pavements, interlayered good and poor-quality concrete.	Experienced operator is required; involves complex signal processing.
Impulse response (ASTM C1740)	Access to only one face is needed; equipment is commercially available; does not require coupling materials; large areas tested in short time.	Experienced operator is required; Thickness limitation of 40 in. (1 m). Comparative results.

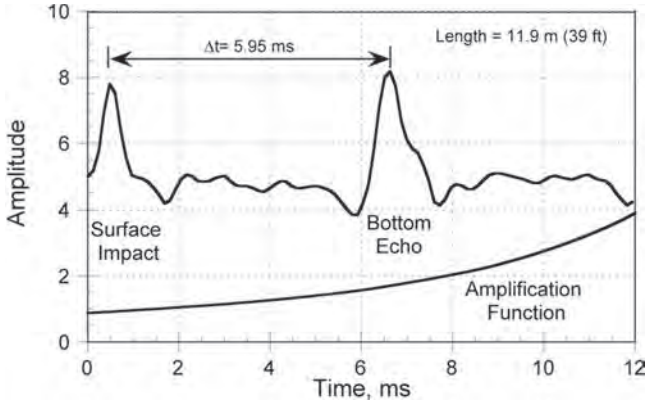

Fig. 3.3.1.1—Example of sonic-echo test result (signal is amplified by function at bottom of graph).

measurements of strain and acceleration became possible, however, it was soon realized that the test results included valuable information about shaft integrity. When integrity methods using hand-held impactors were developed, they become known as low-strain tests to differentiate them from the methods that measured the high-strain stresses caused by the pile driving hammers. Because the high-strain tests are still primarily used as load test methods, they are considered beyond the scope of this committee report. Additional information on high-strain testing can be found in the Deep Foundations Institute Manual on Nondestructive Testing and Evaluation (DFI 2006), Hertlein and Davis (2006), or Davis and Hertlein (1997).

Since the 1960s, test methods based on low-strain stress-wave propagation have been commercially available for the NDT of concrete deep foundations and mass concrete. First developed in France and Holland and closely followed by the United States, they are now routinely specified as quality assurance tools for new pile construction in Western Europe, Northern Africa, and parts of East Asia. In the United States, federally-funded and many state-funded highway projects require quality assurance testing. The use of these methods for evaluation of deep foundations is becoming more common. Continuing advances in electronic hardware and portable computers have resulted in more reliable and faster testing systems that are becoming progressively less influenced by the operator in terms of both testing procedure and analysis of test results.

There are two types of low-strain stress wave methods for evaluation of deep foundations:

1. Reflection techniques (sonic-echo and impulse response)

2. Direct transmission through the concrete (crosshole sonic logging)

3.3.1 *Sonic-echo method*—This method is the earliest of all NDT methods to become commercially available (Paquet 1968; Steinbach and Vey 1975; Van Koten and Middendorp 1981) for deep-foundation integrity or length evaluation. This method is known variously as the seismic-echo, sonic-echo or pile integrity test (PIT) (Rausche and Seitz 1983). Procedures for conducting this type of test are given in ASTM D5882, also called the pulse-echo method (PEM).

3.3.1.1 *Principle*—The sonic-echo method uses a small impact delivered at the head of the deep foundation (pile or shaft), and measures the time taken for the stress wave generated by the impact to travel down the pile and to be reflected back to a transducer, usually an accelerometer, coupled to the pile head. The impact is typically from a small sledge-hammer, having a mass of approximately 2.2 lb (1 kg). The accelerometer captures the motion generated by the impact of the hammer and subsequent wave reflections from within the shaft. The vertical movement of the shaft head due to the impact and the subsequent arrival of the reflected stress wave is captured by a digital data acquisition system that stores the data as a function of time, which is also known as time domain. Figure 3.3.1.1 illustrates the results of a sonic-echo test on a concrete shaft. The time for the stress wave to travel down the shaft and back to the surface is called transit time, and can be determined as shown in Fig. 3.3.1.1.

If the length of the foundation shaft is known and the transit time for the stress wave to return to the transducer is measured, then the wave velocity can be calculated. Conversely, if the velocity is known, then the length can be deduced. Because the velocity of the stress wave is primarily a function of the dynamic elastic modulus and density of the concrete, the calculated velocity can provide information on concrete quality. Where the stress wave has traveled the full length of the shaft, these calculations are based on the formula

$$C_b = \frac{2L}{\Delta t} \tag{3.3.1.1}$$

where C_b is the bar wave speed in concrete; L is the shaft length; and Δt is the transit time of stress wave.

Bar waves are propagating pulse resonances that are set up in long elements when the wavelength of the propagating wave is significantly larger than the bar's cross section dimension. Bar waves propagate at a velocity that is slightly lower than that of P-waves.

Empirical data have shown that a typical range of values for C_b can be assumed, where 15,000 to 15,750 ft/s (3800 to 4000 m/s) would indicate good-quality concrete. The actual strength will vary according to aggregate type and mixture proportions. A project-specific correlation is required to estimate in-place strength from the wave speed (refer to ACI 228.1R).

Where the length of the shaft is known, an earlier-than-expected arrival of the reflected wave means that it has encountered a reflector, which is a change in stiffness or density other than in the toe of the shaft. This may be a break or defect in the shaft, a significant change in shaft cross section, or the point at which the shaft is restrained by a stiffer soil layer. In certain cases, the polarity of the reflected wave, whether positive or negative with respect to the initial impact, can indicate whether the anomaly is due to an increase or decrease of stiffness at the reflective point.

The energy imparted to the shaft by the impact is small, and the damping effect of the soils around the shaft will progressively dissipate that energy as the stress wave travels

down and up the shaft. To increase information from the test, the response signal can be progressively amplified with time. However, caution should be used with this approach because background geo-noise will also be amplified, causing results that can be misleading. Geo-noise is ground-borne noise caused by ocean waves, human activity, storms, seismic events, and similar phenomena.

Depending on the stiffness of the lateral soils, a limiting length-to-diameter ratio (L/d) exists beyond which all the wave energy is dissipated and no response is detected at the shaft head. In this situation, the only information that can be derived is that there are no significant irregularities in the upper portion of the shaft, because any irregularity closer to the head than the critical L/d would reflect part of the wave. This limiting L/d value will vary according to the properties of the adjacent soils, with a typical value of approximately 30:1 for medium stiff clays.

3.3.2 *Impulse-response (mobility) method*—This method was originally developed as a steady-state vibration test in France (Davis and Dunn 1974), where a controlled force was applied to the shaft head by a swept-frequency generator. The vertical shaft response was recorded by geophone velocity transducers, and the input force from the vibrator was continuously monitored. The resulting response curve plotted the shaft mobility (geophone particle velocity divided by vibrator force, v/F) against frequency. The useful frequency range was typically approximately 0 to 2000 Hz.

The evolution of data-processing equipment during the 1980s and 1990s allowed the use of computers on site to transform the shaft response due to a hammer impact (similar to that used in the sonic-echo method) into the frequency domain (Stain 1982; Olson et al. 1990). This reduced the effort required to obtain the mobility as a function of frequency. The impulse response method is also covered by ASTM D5882, where it is called the transient response method (TRM).

Further studies demonstrated that the impulse-response method could be applied to integrity testing of structures other than deep foundations (Davis and Hertlein 1990). The application of impulse response to integrity evaluation of plate-like structures is discussed in 3.2.5.

3.3.2.1 *Principle*—An impact on the shaft head by a small sledge hammer equipped with a force transducer generates a stress wave with a wide frequency content, which can vary from 0 to 1000 Hz for soft rubber-tipped hammers, and from 0 to 3000 Hz or higher for metal-tipped hammers. The load cell measures the force input and the vertical response of the shaft head is monitored by a geophone.

The force and velocity time-domain signals are recorded by a digital acquisition device, and then processed by computer using a fast Fourier transform (FFT) algorithm to convert the data to the frequency domain. At each frequency value, velocity is divided by force to provide the normalized response, transfer function, or frequency response function (FRF), which is displayed as a graph of shaft mobility versus frequency (mobility plot). Appendix A discusses the theoretical aspects of the mobility plot for a deep foundation shaft.

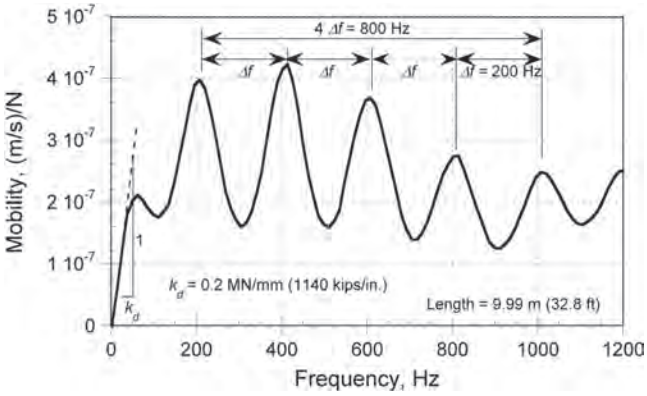

Fig. 3.3.2.1a—Example of impulse-response (mobility) plot for test of pile.

An example of a mobility plot for a foundation shaft is given in Fig. 3.3.2.1a. This response curve consists of two major portions, which contain the following information:

a) At low frequencies (less than 100 Hz), lack of inertial effects cause the shaft-soil composite system to behave as a spring, which is shown as a linear increase in amplitude with increasing frequency. The slope of this portion of the mobility plot is known as the compliance or flexibility, and the inverse of flexibility is the dynamic stiffness. The dynamic stiffness, which is a property of the shaft-soil system, can be used to assess shafts on a comparative basis, either to assess uniformity or as an aid to selecting a representative shaft for full-scale load testing by either static or dynamic means.

b) The peaks in the higher-frequency portion of the mobility plot are due to longitudinal resonances of the shaft. The resonant frequencies are a function of the shaft length and the degree of shaft toe anchorage and their relative amplitude is a function of the lateral soil damping. The frequency difference between adjacent peaks is constant and is related to the length of the shaft and the wave speed of the concrete according to Eq. (A.1) in Appendix A. The mean amplitude of the resonance portion of the curve is a function of the impedance of the shaft, which depends in turn on the shaft cross-sectional area, the concrete density, and the bar wave propagation velocity C_b (refer to Appendix A).

As with the sonic-echo test, when the shaft length is known, a shorter apparent length measurement indicates the presence of an anomaly. Appendix A describes how additional information can be derived from the mobility-frequency plot, such as the shaft cross section and dynamic stiffness, which can help in differentiating between an increase and reduction in cross section.

Figure 3.3.2.1b shows a mobility plot of a 30.5 ft (9.3 m) long shaft with similar soil conditions to the shaft in Fig. 3.3.2.1a, except for a necked section at 10.2 ft (3.1 m). The reflection from the shaft base at 30.5 ft (9.3 m) depth is clearly visible on the plot, indicated by resonance peaks at the constant frequency spacing of 215 Hz. The frequency spacing of 645 Hz between the two more prominent peaks corresponds to the reflection from the necked section at a depth of 10.2 ft (3.1 m).

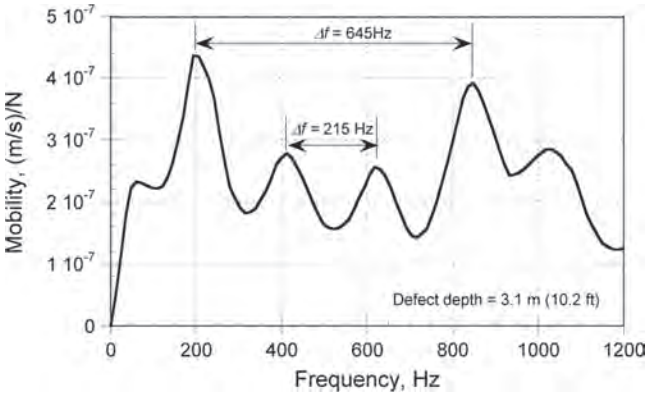

Fig. 3.3.2.1b—Impulse-response (mobility) plot of pile with necked section 10.2 ft (3.1 m) below top.

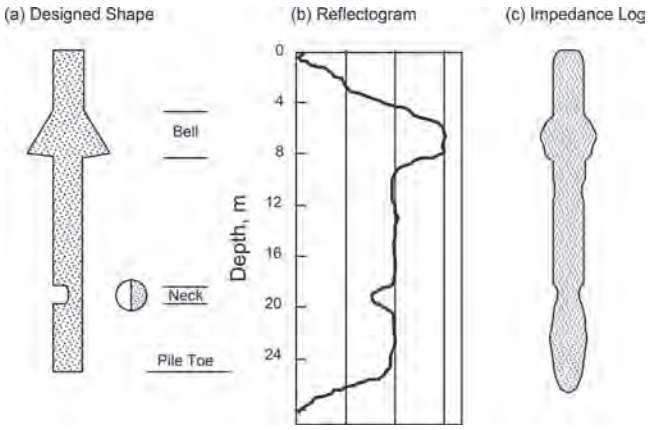

Fig. 3.3.3.1—(a) Planned defects in experimental pile; (b) reflectogram obtained by signal processing of sonic-echo data; and (c) impedance log obtained by combining information from reflectogram and characteristic impedance obtained from impulse-response analysis.

In common with the sonic-echo test, a relatively small amount of energy is generated by the hammer impact, and soil damping effects limit the depth from which useful information may be obtained. However, even where no measurable shaft base response is present, the dynamic stiffness is still a useful parameter for comparative shaft assessment.

3.3.3 *Impedance logging*—Another approach to interpreting the responses from a combination of both sonic-echo and impulse-response methods is impedance logging (Paquet 1991). In this technique, the information from the amplified time-domain response of the sonic echo is combined with the characteristic impedance of the shaft measured with the mobility test to create an image of the variation in shaft impedance with depth.

3.3.3.1 *Principle*—The force applied to the head of the shaft by the surface reflection method is a brief transient event—1 to 3 milliseconds—that generates an elastic wave that propagates down the shaft. This wave collects information about changes in shaft impedance as it proceeds downward, and is then reflected back to the shaft head. The only useful reflections in the analysis process are those that arrive after the initial surface disturbances from the impact (Rayleigh waves) have dissipated.

The reflectogram obtained from the sonic-echo test does not indicate the relative size of the irregularity that caused the reflection. However, it is possible with modern recording equipment to combine the information from wave reflection with the impedance properties of the shaft. Measurements of force and velocity response are stored as time-based data, with a very wide band-pass filter and rapid sampling. In the reflectogram, a defect extending across the entire shaft cross section (zero impedance) is equivalent to 100 percent reflection, whereas an infinitely long shaft with no defects would give zero reflection.

If either a defect or the shaft tip is at a considerable distance from the shaft head, the reflected amplitude is reduced by damping within the shaft. With uniform lateral soil conditions, this damping function has the form $e^{-}\sigma^{L}$, where L is the shaft length and σ is the damping factor (refer to Appendix A). The reflectogram can be corrected for the effects of damping by using an amplification function that yields a high-amplitude response over the total shaft length, similar to the treatment of sonic-echo data. Figure 3.3.3.1 shows an example of a reflectogram that has been corrected in this way.

The analysis of the mobility plot from the impulse-response test confirms shaft length, gives the shaft-soil system dynamic stiffness, and gives the characteristic shaft impedance I as

$$I = \rho_c A_c C_b \qquad (3.3.3.1)$$

In addition, Davis and Dunn (1974) showed that finite element simulation of the tested shaft and its surrounding soil can be carried out most efficiently in the frequency domain. The reflectogram and the characteristic impedance can then be combined to produce a trace called the impedance log (Fig. 3.3.3.1(c)). The output of this analysis is in the form of a vertical section through the shaft, giving a calculated visual representation of the effective pile shape. The final result can be adjusted to eliminate varying soil reflections using the simulation technique.

Field testing equipment should meet the following:

a) Hammer load cell and the velocity transducer or accelerometer should be correctly calibrated, generally within 6 months before testing.

b) Digital data acquisition and storage equipment should be used to allow subsequent analysis.

c) Both time and frequency-domain test responses should be stored.

3.3.4 *Crosshole sonic logging*—The crosshole sonic logging (CSL) method overcomes the depth limitation of the sonic-echo and mobility methods, and is appropriate for use on deep drilled shafts and mass concrete foundations such as slurry trench walls, dams, and machinery bases (Levy 1970; Davis and Robertson 1975; Baker and Khan 1971). This method is based on the principle of ultrasonic through transmission, as discussed in 3.2.1, and its use for deep foundations is covered by ASTM D6760.

3.3.4.1 *Principle*—This is a method that requires a number of parallel metal or plastic tubes to be placed in the structure before concrete placement, or core holes to be drilled after the concrete has gained sufficient strength to permit drilling. Typically, a transmitting transducer initially placed at the bottom of one tube emits an ultrasonic pulse that is detected by a receiving transducer at the bottom of a second tube. A recording unit measures the time taken for the ultrasonic pulse to pass through the concrete between the tubes. The transducers are watertight sealed units, and the tubes are filled with water to provide coupling between the transducers and the concrete. For the pulse to be transmitted between the concrete and transducers, mechanical bond is required between the concrete and the outer walls of the tubes.

The transducer cables are withdrawn over an instrumented wheel that measures the cable length and, thus, transducer depth. Alternatively, the cables can be marked along their lengths so that the transducer depths are known. Continuous pulse measurements are made during withdrawal at height increments ranging from 0.5 to 2 in. (10 to 50 mm), providing a series of measurements that can be printed out to create a vertical profile of the material between the tubes. A typical test result for a specific commercial system is shown in Fig. 3.3.4.1. The presence of an anomaly is indicated by an increase in the time of flight of the signal or the complete absence of a received signal.

As discussed in 3.2, the ultrasonic pulse velocity (UPV) is a function of the density and dynamic elastic constants of the concrete. If the signal path length is known and the transit time is recorded, the apparent UPV can be calculated to provide a guide to the quality of the concrete. A reduction in elastic modulus results in a lower UPV. If the path length is not known, but the tubes are reasonably parallel, the continuous measurement profile will clearly show any sudden changes in transit time caused by a lower pulse velocity due to poor-quality material, such as contaminated concrete or inclusions. Voids will have a similar effect by forcing the pulse to detour around them by diffraction, thus increasing the path length and the transit time.

Although the amplitude of the received pulse is also likely to be affected by anomalies within the concrete, it can also be affected by other factors, such as the transducers location within the tubes, the quality of the bond between the tubes and the concrete, the distribution and orientation of the coarse aggregate within the concrete, and the amplitude of the pulse emitted by the transmitter. Reliance solely on variations in signal amplitude as an indication of concrete anomalies is therefore prone to error.

By varying the geometric arrangement of the transducers, the method can resolve the vertical and horizontal extent of such irregularities and locate cracks or discontinuities. This additional information can help the engineer decide whether the irregularity is merely an insignificant flaw that will not impact the performance or durability of the foundation or a defect that could have a significant adverse effect on shaft capacity or durability.

This method, which provides a direct measurement of foundation depth, can be used to assess the quality of the interface between the shaft base and the bedrock if the access holes are extended below the base. A major limitation of this method is the requirement to install access tubes either before concrete placement or by core drilling afterward. One major advantage is that the method has no practical depth limitation, unlike the surface reflection methods.

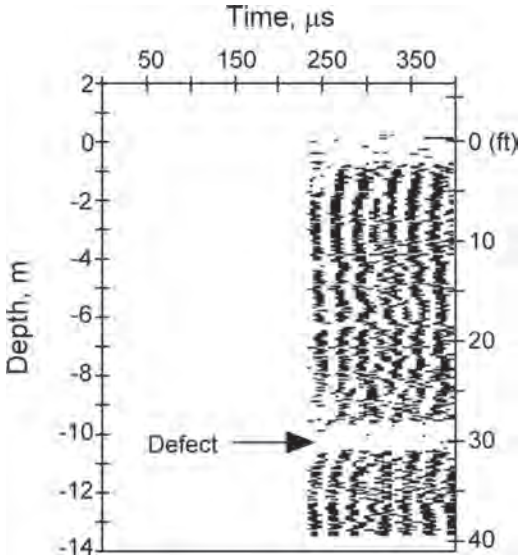

Fig. 3.3.4.1—Example of crosshole sonic log. Absence of signal arrival at depth of approximately 33 ft (10 m) indicates presence of potential defect.

The information obtained is limited to the material immediately between pairs of tubes. Therefore, in piles or drilled shafts, the access tubes should be arranged as close to the shaft periphery as possible in a pattern that allows the maximum coverage of the concrete between them. Very little useful information will be obtained about increases or decreases in shaft cross section in regions outside the direct paths between all possible pair combinations of the access tubes.

3.3.5 *Parallel-seismic method*—All of the aforementioned methods depend on clear access to the head of the foundation shaft, making them the easiest and most practical to perform during the construction phase, as foundation heads may later be inaccessible. The parallel-seismic method was developed specifically for situations arising after the foundation has been built upon, as in the evaluation of older, existing structures where direct access to the shaft head is no longer possible without some demolition or material removal (Davis 1995).

3.3.5.1 *Principle*—A small-diameter (typically 6 to 8 in. [150 to 200 mm] in size) access borehole is drilled into the soil parallel and close to the foundation to be tested. The borehole should extend beyond the known or estimated depth of the foundation. The borehole is lined normally with a plastic tube to retain water, which serves as an acoustic couplant, and allows the transducer unrestricted access to the bottom of the borehole. The inside diameter of the tube is typically 2 to 3 in. (50 to 75 mm), and the tube is fully grouted into the borehole with bentonite or material with a modulus similar to that of the surrounding soil.

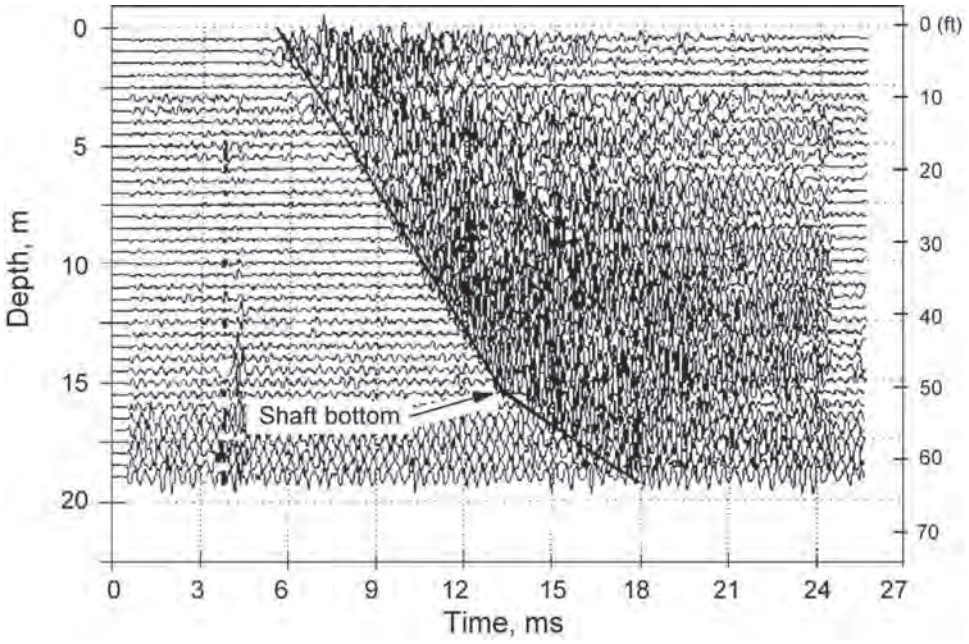

Fig. 3.3.5.1—Example of results from parallel-seismic test. Depth of pile shaft is indicated by change in slope of line representing arrival time of stress pulse as a function of depth.

An acoustic receiving transducer, or hydrophone, is placed in the top or the bottom of the tube, and the structure is struck as close to the head of the foundation as possible using a hammer equipped with an electronic trigger. A portion of the energy traveling down the foundation element is refracted into the soil and the hydrophone will respond to the arrival of the refracted portion of the stress pulse. The signal from the hammer impact triggers the data acquisition system, which records the time domain signal from the hydrophone. The received signal allows determination of the time taken for the stress wave to travel through the foundation and the adjacent soil to the hydrophone. The hydrophone is then lowered or raised in uniform increments and the process repeated at each stage, with the impact at the same point each time. The recorded time domain waveforms are stacked vertically in a single plot of depth versus time (waterfall plot), with each waveform plotted at the corresponding depth of the hydrophone, as shown in Fig. 3.3.5.1. A best-fit straight line is drawn through the times corresponding to pulse arrival for each hydrophone position.

The velocity of the wave will be lower through soil than the foundation. If the access tube is reasonably parallel to the foundation, the effect of the soil between the tube and the pile shaft will be constant. Transit time, however, will increase proportionally as the depth of the hydrophone increases. When the receiver has passed beyond the foundation base, the transit time of the signal will increase due to the lower velocity of the additional intervening soil, and the lines linking signal arrival points on the graph show a distinct change in slope at the level of the foundation base. Similarly, any significant discontinuity or inclusion in the foundation will force the signal to detour around it, increasing the path length and transit time, which results in a deviation of the transit time from the best-fit straight line.

3.3.5.2 *Interpretation*—The results of low-strain stress wave methods are affected by the size and location of the irregularity within the foundation. A small inclusion or reduction in cross section near the top of a shaft being tested with one of the impulse methods or close to one of the access tubes in the crosshole sonic logging (CSL) test can appear as a more significant anomaly in the data than a similar-sized feature further away. Often, a small irregularity will have no significant effect on foundation capacity or durability, making it uneconomical and unnecessary to repair. Using the word "defect" to describe all irregularities is therefore misleading, and creates an unnecessarily negative impression for evaluation. The Test and Evaluation Committee of the DFI therefore recommends that interpretation of integrity test data be subjected to a three-level classification (DFI 2006):

1. Anomaly—Any irregular feature identified in the NDT graphic results that could be caused by testing instrumentation, like noise, or from any other means used to perform the test, for example access tube debonding in CSL, or to the shaft itself. The NDT practitioner is responsible for gathering and analyzing all the relevant data and attempting to resolve every anomaly before it is declared a flaw or defect.

2. Flaw—Any deviation from any combination of the planned shape, size, or material of the shaft.

3. Defect—A flaw caused by either the size or location that might detract from the shaft's intended performance or durability. The geotechnical engineer and the structural engineer are jointly responsible for deciding which flaw constitutes a defect.

3.3.6 *Advantages and limitations*—Table 3.3.6 summarizes the advantages and limitations of stress-wave methods for deep foundations.

Table 3.3.6—Advantages and limitations of stress-wave methods for deep foundations

Method	Advantages	Limitations
Surface reflection methods		
Sonic-echo	No preplaced tubes. Portable equipment. Rapid.	Can confuse necking and bulging. Does not measure diameter. May be unable to measure length or detect irregularities in lower portions of shafts with *L*/*d* greater than approximately 30:1.
Impulse-response (mobility)	No preplaced tubes. Stiffness measurement. Portable equipment. Rapid.	Results interpretation is complex. Similar limitations on geometry of shafts tested as sonic-echo.
Impedance logging	Same as for mobility test, plus effective shape of shaft derived from analysis.	Requires very good test data for accurate analysis. Full analysis requires experience, and cannot yet be completed on-site at time of test.
Direct transmission methods		
Sonic logging	Relatively fast. Detection of irregularities between tubes is more accurate than in surface reflection tests. Performance is not limited by depth.	Preplaced tubes or coring required. May not detect irregularities at edge of shaft.
Parallel-seismic	Relatively fast. Foundations under existing structures can be tested. Not affected by soil damping as much as surface reflection methods.	Requires testing hole to be bored adjacent to the foundation that is to be inspected. May not detect defects that are not complete discontinuities.

3.4—Nuclear methods

3.4.1 *Introduction*—Nuclear methods for nondestructive evaluation of concrete is subdivided into two groups, depending on the type of radiation used, which is either gamma rays or neutrons. The gamma-ray-based techniques include radiometric methods and radiographic methods. All involve gaining information about a test object due to interactions between the incident radiation and the material in the test object. A review of the early developments in the use of nuclear methods was presented by Malhotra (1976). Their developments up to the 1990s were reviewed by Mitchell (2004). Examples of further developments in the 2000s, given by Mariscotti et al. (2009), use radioactive materials and require test personnel to have specialized safety training and licensing.

3.4.1.1 *Radiometry*—Radiometry is used to assess the density of fresh or hardened concrete by measuring the intensity of electromagnetic radiation (gamma rays) that passes through the concrete. The radiation is emitted by a radioactive isotope, and the radiation passing through the concrete is sensed by a detector. The detector converts the received radiation into electrical pulses, which can be counted or analyzed by means of electronic devices (Mitchell 2004). Radiometry can be further subdivided into two procedures. One is based on measurement of gamma rays after transmission directly through concrete, and the second is based on measurement of gamma rays reflected, or backscattered, from within the concrete. These procedures are analogous to the ultrasonic through-transmission method and the pitch-catch method using stress waves.

3.4.1.2 *Radiography*—Radiography involves the use of the radiation passing through the test object to produce a photograph of the internal structure of the concrete. Typically, a radioactive source is placed on one side of the object and special photographic film or a reusable image plate is placed on the opposite side to record the intensity of radiation passing through the object. The higher the intensity of the radiation, the greater the exposure of the film or the stimulation of phosphors in an image plate. This method is identical to that used to produce medical X-ray images.

3.4.1.3 *Neutron*—Neutron sources can be used to measure the amount of moisture in concrete and to determine the elemental composition of concrete. The assessment of moisture is based on the knowledge that neutrons are strongly scattered by hydrogen atoms that are part of water molecules. In the usual arrangement, a neutron source and one or more neutron detectors are placed on a concrete surface with the latter being well-shielded from the source. Neutrons scattered back from within the concrete are registered by the detector(s) (refer to 3.4.3). In the second application, the elemental composition of concrete is determined by measuring the characteristic wavelength of the gamma rays emitted by the atoms in the concrete when these are hit by neutrons. In this case, gamma-ray spectrometers, which are detectors sensitive to the difference in wavelengths, are used in conjunction with a neutron source (Collico Savio et al. 1995; Saleh and Livingston 2000). A less practical alternative, which involves irradiating concrete samples in a nuclear reactor, is termed neutron activation analysis as described by Malhotra (1976).

3.4.2 *Direct transmission radiometry for density*—Direct transmission techniques can be used to detect reinforcement. The more common use of the technique, however, is to measure the in-place density both in fresh and hardened concrete (ASTM C1040/C1040M). Structures made with high-density (heavyweight) concrete or roller-compacted concrete are cases where this method is of particular value.

3.4.2.1 *Principle*—The direct transmission radiometric method is, as stated, analogous to the ultrasonic through-transmission technique discussed in 3.2. The radiation source is placed on one side of the concrete element to be tested and the detector is placed on the opposite side. For testing fresh concrete, the source is typically embedded to the concrete and the detector is located on the surface or embedded at a fixed distance from the source. As the radiation passes through the concrete, a portion is scattered by free electrons (Compton scattering) and another portion is absorbed by atoms. The amount of Compton scattering depends on the density of the concrete and the amount of absorption depends on chemical composition (Mitchell 2004). If the source-detector spacing and the concrete thickness are held

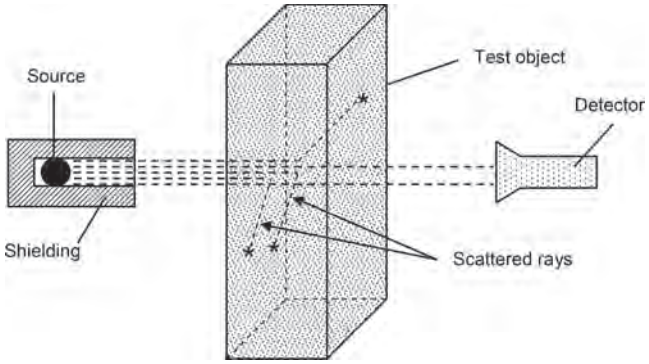

Fig. 3.4.2.2a—Direct transmission radiometry with source and detector external to test object.

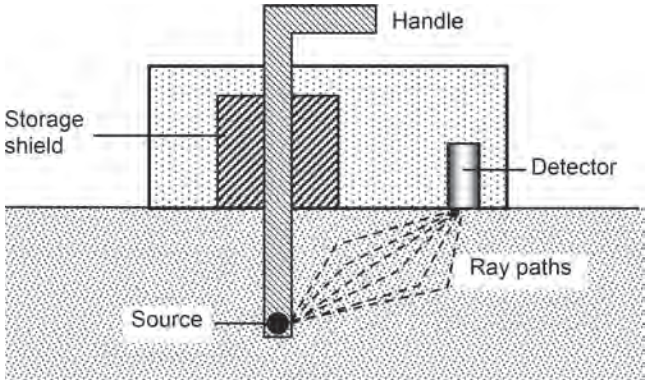

Fig 3.4.2.2b—Schematic of direct transmission nuclear gauge.

constant, a decrease (or increase) in concrete density leads to a change in the intensity of the detected radiation.

3.4.2.2 *Instrumentation*—Figure 3.4.2.2a shows the arrangement of source and detector for direct measurement through a hardened concrete member. This arrangement could also be used for testing fresh concrete with allowance made for the effects of the formwork material. The most widely used source is the radioactive isotope cesium-137 (^{137}Cs). The common detector is a Geiger-Müller tube, which produces electrical pulses when radiation enters the tube. Other detectors can be scintillation crystals that convert incident radiation into light pulses.

Figure 3.4.2.2b is a schematic of a commercially available nuclear transmission gauge that is used to test fresh concrete by pushing the source assembly into the concrete. It can also be used in hardened concrete by drilling a hole and inserting the source assembly. The equipment is portable and provides an immediate readout of the results. Most of the available units were developed for monitoring soil compaction and measuring the in-place density of asphalt concrete.

The VUT density meter was developed specifically for measuring the density of fresh concrete (Hönig 1984). Figure 3.4.2.2c is a schematic of this device. The source can be lowered up to a depth of 8 in. (200 mm) into a hollow steel needle that is pushed into the fresh concrete. A spherical lead shield suppresses the radiation when the source is in its retracted position. Detectors are located beneath the treads

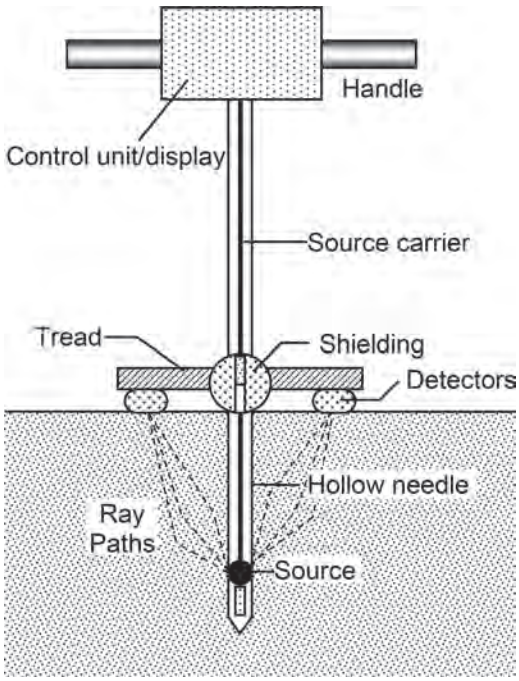

Fig. 3.4.2.2c—Schematic of nuclear gauge for measuring density of fresh concrete (based on Hönig [1984]).

used to push the needle into the concrete. The unit is claimed to have a resolution of 0.6 lb/ft^3 (10 kg/m^3) (Hönig 1984).

The direct transmission gauges mentioned previously provide a measurement of the average density between the source and detector. Figure 3.4.2.2d is a schematic of a two probe source/detector system for measuring the density of fresh concrete as a function of depth (Iddings and Melancon 1986). The source and detector are moved up and down within metal tubes that are pushed into the fresh concrete, making it possible to measure density as a function of depth.

ASTM C1040/C1040M provides procedures for using nuclear methods to measure the in-place density of fresh or hardened concrete. A key element in the procedure is determining a calibration curve for the instrument by making test specimens of different densities and determining the gauge output for each specimen. The gauge output is plotted as a function of the density and a best-fit curve determined. The procedure for using the direct transmission method to measure density of fresh concrete is given in ASTM C1040/C1040M (Procedure A).

3.4.3 *Backscatter radiometry for density*—Backscatter techniques are particularly suitable for applications where a large number of in-place measurements are required. Because backscatter measurements are affected by the top 1.6 to 4 in. (40 to 100 mm), the method is best suited for measurement of the surface zone of a concrete element. A good example of this method is monitoring the density of bridge deck overlays. Noncontacting equipment is available to use for continuously monitoring concrete pavement density during slipforming operations.

3.4.3.1 *Principle*—When measuring density by backscatter, the radiation source and the detector are placed on the same side of the sample (analogous to pitch-catch method for

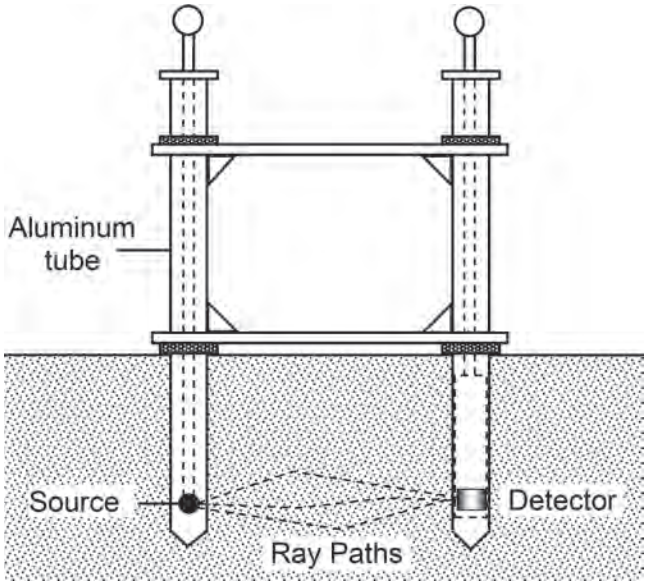

Fig. 3.4.2.2d—Schematic of direct transmission nuclear gauge for measuring density of fresh concrete at different depth (adapted from Iddings and Melancon [1986]).

stress waves discussed in 3.2). The difference between backscatter radiometry and direct transmission radiometry is that, in the former case, the detector only receives gamma rays that are scattered within the concrete rather than registering both scattered and direct radiation. Scattered rays have lower energy than the direct (primary) rays and are produced when a gamma-ray photon collides with an electron in an atom. Part of the photon energy is imparted to the electron and a new photon emerges, traveling in a different direction with lower energy, which is a process known as Compton scattering (Mitchell 2004).

The procedure for using the backscatter method to measure density of fresh or hardened concrete is given in ASTM C1040/C1040M (Procedure B). Like direct transmission measurements, it is necessary to establish a calibration curve before using a nuclear backscatter gauge to measure in-place density.

3.4.3.2 *Instrumentation*—Figure 3.4.3.2 is a schematic of a backscatter nuclear gauge for density measurement. Many commercial gauges are designed so that they can be used in either direct transmission or backscatter mode. To operate the gauge in backscatter mode, the source is positioned so that it is located on the surface of the concrete. Shielding is provided to prevent radiation traveling directly from the source to reach the detector.

Specialized versions of backscatter equipment have been developed. Two of particular interest are described in 3.4.3.1.1 and 3.4.3.1.2.

3.4.3.1.1 *ETG probe*—The electronic thickness gauge (ETG) probe was developed in Denmark to use backscatter measurements for estimating density variation at different depths in a medium. The technique involves determination of the intensity of backscattered gamma radiation as a function of energy level. A beam of parallel (collimated) gamma rays is used and multiple measurements are made

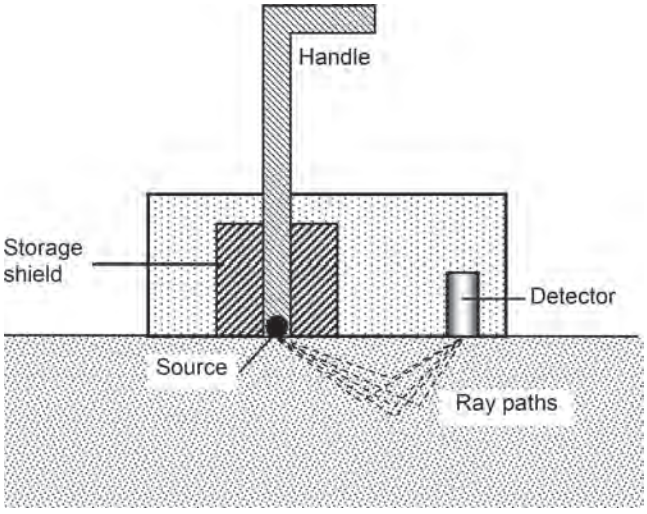

Fig. 3.4.3.2—Schematic of backscatter nuclear density gauge.

with the beam at slightly different angles of penetration. By comparing the radiation spectra for the multiple measurements, information can be obtained about the density in a specific layer of the concrete. In addition to permitting measurement of density at discrete layers, the ETG probe also permits density measurements at greater depths of up to 6 in. (150 mm) than are possible by ordinary backscatter gauges (Berg et al. 1989).

3.4.3.1.2 *Consolidation monitoring device*—This equipment was developed for continuous monitoring of pavement consolidation during slipform construction (Mitchell et al. 1979). The device is mounted on the rear of a highway paving machine and traverses across the finished pavement at a height of approximately 1 in. (25 mm) above the pavement surface. An air gap compensating device allows for air gap variations of up to 0.4 in. (10 mm). The device measures the average density within the top 4 in. (100 mm) of the pavement.

3.4.4 *Radiography*—Radiography provides a means of obtaining a radiation-based photograph of the interior of concrete because denser materials block more of the radiation. From this photograph, the location of reinforcement, voids in concrete, or voids in grouting of post-tensioning ducts can be identified. When the radiation source produces gamma rays, the method is called gammagraphy, but in this report, the term "radiography" is used both for X-ray and gamma ray sources.

3.4.4.1 *Principle*—A radiation source is placed on one side of the test object and a beam of radiation is emitted. Alternatively, the radiation source can be placed in a hole drilled into the concrete (Mariscotti et al. 2009). As the radiation passes through the member, it is attenuated by differing amounts, depending on the density and thickness of the material that is traversed. The radiation that emerges from the opposite side of the object strikes a special photographic film (Fig. 3.4.4.1). The film is exposed in proportion to the intensity of the incident radiation. When the film is developed, a two-dimensional (2-D) visualization (a photograph) of the interior structure of the object is obtained. The

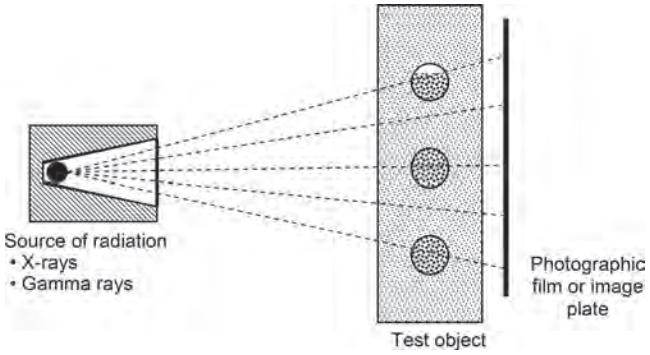

Fig. 3.4.4.1—Schematic of radiographic method.

presence of a high-density material, such as reinforcement, is shown on the developed film as a light area, and a region of low density, such as a void, is shown as a dark area.

An image plate instead of photographic film can also be used. An image plate is composed of a phosphor screen that captures the energy of the radiation passing through the test object. A laser beam is then used to convert the stored energy to a luminescent signal that is captured and stored as a 2-D digital array. The digital information can be subjected to signal processing to obtain quantitative estimates of, among other things, loss of cross section of reinforcement due to corrosion (Mariscotti et al. 2009). If images are obtained with the source in different positions, accurate three dimensional (3-D) reconstructions of the reinforcement can be generated through triangulation by projecting an array of calibrated reference marks onto the plates (Mariscotti et al. 2009; Thieberger et al. 2009).

The British Standards Institute (BSI) has adopted a standard for radiographic testing of concrete based on BS 1881-205. The standard provides recommendations for investigators considering radiographic examinations of concrete (Mitchell 2004).

3.4.4.2 *Instrumentation*—In X-radiography, the radiation is produced by an X-ray tube (Mitchell 2004). The penetrating ability of the X-rays depends on the operating voltage of the X-ray tube. In gammagraphy, a radioactive isotope is used as the radiation source. The selection of a source depends on the density and thickness of the test object and on the exposure time that can be tolerated. The most energetic source is cobalt-60 (Co), which can be used to penetrate up to 20 in. (500 mm) of concrete. For members with thickness of 10 in. (250 mm) or less, iridium-192 (Ir) or cesium-137(Cs) can be used based on BS 1881-205. The film type will depend on the thickness and density of the member being tested. The source Ir is the least energetic of these three sources and can be used to image a concrete thickness up to 12 in. (300 mm) using approximately 15 to 30 minutes of exposure time (Mariscotti et al. 2009). Despite these limitations, Ir is preferred because it requires the least amount of shielding material and can be effectively used in most applications by inserting the source inside a hole drilled in the concrete (Mariscotti et al. 2009).

Most field applications have used radioactive sources because of their greater penetrating ability (higher energy radiation) compared with X-rays. A system developed in France uses an electron linear accelerator to produce very-high-energy X-rays that can penetrate up to 40 in. (1 m) of concrete. This system was developed for the inspection of prestressed members to establish the condition and location of prestressing strands and to determine the quality of grouting in tendon ducts (Mitchell 2004). Note that the technique is difficult to apply in the field and beam hardening effects may hide voids (Im et al. 2010). Beam hardening refers to the process whereby the average energy level of an X-ray beam increases with penetration as the lower energy photons are filtered out.

3.4.5 *Gamma-gamma logging of deep foundations*—This technique is used to evaluate the integrity of drilled shaft and slurry wall foundations by measuring the density of the concrete surrounding access tubes or holes in the deep foundations. Gamma-gamma logging uses a radioactive source and a radiation detector that may be either in separate units (direct transmission) or housed in the same unit (backscatter) (Preiss and Caiserman 1975; Davis and Hertlein 1994).

3.4.5.1 *Principle*—The most common method is by backscatter, with the source-detector unit (probe) lowered down a single dry plastic access tube, and raised at a uniform rate to the surface. Low-density zones, such as soil inclusions, within 2 to 4 in. (50 to 100 mm) from the probe will decrease the radiation count because less radiation is backscattered than in a zone of intact concrete. A limitation of the method is the need for stronger radiation sources to increase the zone of influence of the probe around the tube.

The effect of different access tube materials on relative gamma-ray count is demonstrated in Fig. 3.4.5.1, which shows plots of radiation counts from an experimental drilled shaft with four access tubes: two of plastic and two of steel (Baker et al. 1993). The response from the shaft constriction at 36 to 39 ft (11 to 12 m) is attenuated by the steel tubes. The figure also shows that a small elliptical inclusion at 13 ft (4 m) is not detected in any of the traces, demonstrating the limitation of the method to locate small flaws, unless they are located close to the access tubes.

When gamma-gamma logging is used in the direct transmission mode in parallel tubes (Preiss 1971), the data can be analyzed in a similar manner to that from crosshole sonic logging (3.3). This technique requires a strong source and dedicated equipment; for these latter reasons, it is difficult to use in North America.

3.4.6 *Advantages and limitations*—Table 3.4.6 summarizes the advantages and limitations of the nuclear methods. Direct transmission radiometry, which requires a drilled hole in hardened concrete, provides rapid determination of the in-place density of concrete. The equipment is reasonably portable, making it suitable for use in the field. Minimal operator skills are required to make the measurements. For the commercially available equipment, the source/detector separation is limited to a maximum of approximately 12 in. (300 mm). The most commonly available equipment, which measures an average density between the immersed source

and the surface detector, is incapable of identifying areas of low compaction at specific depths. All immersed-probe techniques for fresh concrete have another drawback in that the immersion of the probe may have a localized influence on the concrete being measured. Test results may be affected by the presence of reinforcing steel located near the source-detector path.

Backscatter tests can be used on finished surfaces where direct transmission measurements would be impractical or disruptive. The equipment is portable and tests can be conducted rapidly. The precision of backscatter gauges, however, is less than that of direct transmission devices. ASTM C1040/C1040M requires that a suitable backscatter gauge for density measurement should result in a single-operator standard deviation of less than 1 lb/ft^3 (16 kg/m^3); for a suitable direct-transmission gauge, the single-operator standard deviation should be less than 0.5 lb/ft^3 (8 kg/m^3). According to ASTM C1040/C1040M, backscatter gauges are typically influenced by the top 3 to 5 in. (75 to 125 mm) of material. The top 1 in. (25 mm) determines 50 to 70 percent of the count rate and the top 2 in. (50 mm) determines 80 to 95 percent of the count rate. When the material being tested is homogenous, this inherent characteristic of the method is not significant. When a thin overlay, however, is placed on existing concrete, this effect has to be considered in interpreting the results. Also, the presence of reinforcing steel within the influence zone will affect the count rate.

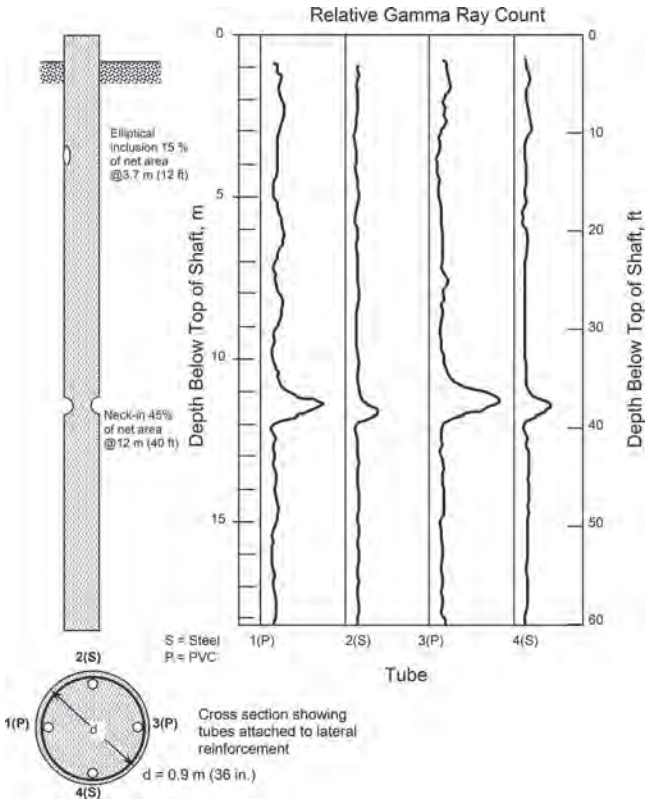

Fig. 3.4.5.1—Gamma-gamma backscatter log on experimental shaft with planned defects (Baker et al. 1993).

Radiographic methods allow the possibility of seeing some of the internal structure of a concrete member where density variations exist. Although both gamma ray and X-ray sources can be used for radiography, X-ray equipment is comparatively expensive and cumbersome for field application. Because of this, less costly and more portable gamma-ray equipment is generally chosen for field use. X-ray equipment, however, has the advantage that it can be turned off when not in use. In contrast, gamma rays are emitted continuously from a radioactive source requiring heavy shielding to protect personnel. In addition, special X-ray equipment, such as electron linear accelerators, can produce more energetic radiation than radioactive sources, which permits the inspection of thicker members or the use of shorter exposure times. When image plates are used instead of film, digital signal processing can be used to extract quantitative information about the internal conditions. By taking multiple images with difference source-detector orientations, tomographic images of the interior structure can be created.

The main concern in the use of all nuclear methods is safety. In general, personnel who perform nuclear tests should obtain a license from the appropriate governmental agency (Mitchell 2004). Testing across the full thickness of a concrete element is particularly hazardous and requires extensive precautions, skilled personnel, and highly specialized equipment. Radiographic procedures require evacuation of the site where measurements are carried out by persons not involved in the actual testing. The use of X-ray equipment poses an additional danger due to the high voltages used. There are limits on the thicknesses of the members that can be tested by radiographic methods. For gamma-ray radiography, the maximum thickness is approximately 20

Table 3.4.6—Advantages and limitations of nuclear methods

Method	Advantages	Limitations
Direct transmission radiometry	Portable equipment available for determination of in-place density. Minimal operator skill is required.	Operators must be licensed. Available equipment limited to path lengths less than 12 in. (300 mm). Requires access to inside of member or opposite faces.
Backscatter radiometry	Requires access only to surface of test object and is suitable for fresh or hardened concrete. Equipment is portable and testing is rapid.	Operators must be licensed. Precision of density measurements is lower than direct transmission. Measurement is affected by near-surface material and is sensitive to chemical composition.
Radiography	Provides view of the internal structure of the test object. Use of image plates allows for digital signal processing to extract more information about the internal structure. Tomography of reinforcement in large columns and beams can be achieved introducing portable ^{192}Ir sources in holes drilled in the concrete.	Operators must be licensed and highly skilled. X-ray equipment is bulky and expensive. Difficult to identify cracks perpendicular to radiation beam. Gamma-ray penetration limited to 20 in. (500 mm) of concrete. Access to opposing faces is required.

in. (500 mm) because thicker members require unacceptably long exposure times. Tomography of reinforcement in large columns and beams can be achieved in most cases by introducing 192 Ir sources in holes drilled in the concrete. Radiography is not very useful for locating crack planes perpendicular to the radiation beam.

3.5—Magnetic and electrical methods

Knowledge about the quantity and location of reinforcement is needed to evaluate the strength of reinforced concrete members. Knowing whether there is active corrosion of reinforcement is necessary to assess the need for remedial actions before structural safety or serviceability is jeopardized. This section discusses some of the magnetic and electrical methods used to gain information about the layout and condition of embedded steel reinforcement (Bungey et al. 2006; Lauer 2004; Carino 2004b). Devices to locate reinforcing bars and estimate the depth of cover are known as covermeters, reinforcing bar locators, or pachometers. In this report they will be called covermeters.

Electrical methods are used to evaluate corrosion activity of steel reinforcement. As is the case with other nondestructive test (NDT) methods, an understanding of the underlying principles of these electrical methods is needed to obtain meaningful results. In addition, an understanding of the factors involved in the corrosion mechanism is essential for reliable interpretation of data from this type of testing. The likelihood of corrosion activity can be monitored using the half-cell potential technique, where the potential for high corrosion rate can be inferred from the concrete resistivity and information on the rate of corrosion can be obtained from linear-polarization methods. Sections 3.5.2 through 3.5.4 provide basic information about these methods. Actual testing and interpretation of test results should, however, be completed by experienced personnel.

The magnetic flux leakage method may be able to detect fractures in prestressing steel.

3.5.1 *Covermeters*—As is common with other NDT methods used to infer conditions within concrete, covermeters measure the depth of cover by monitoring the interaction of the reinforcing bars with some other process. For most covermeters, the interaction is between the bars and a low-frequency electromagnetic field. The basic relationships between electricity and magnetism are key to understanding the operation of covermeters. One important principle is electromagnetic induction, which is an alternating magnetic field intersecting an electrical circuit that induces an electrical potential in that circuit. According to Faraday's law, the induced electrical potential is proportional to the rate of change of the magnetic flux through the area bounded by the circuit (Serway 1983).

Commercial covermeters can be divided into two classes: those based on the principle of magnetic reluctance and those based on eddy currents. Their differences are summarized in 3.5.1.1 and 3.5.1.2 (Carino 1992).

3.5.1.1 *Magnetic reluctance meters*—When electrical charge flows through an electrical coil, a magnetic field is created and a magnetic flux composed of magnetic lines is set up between the magnetic poles of the coil. This leads to a magnetic circuit, in which the magnetic flux between poles is analogous to the current in an electrical circuit (Fitzgerald et al. 1967). The resistance to creation of magnetic flux is called reluctance, which is analogous to the resistance to flow of charge (current) in an electrical circuit.

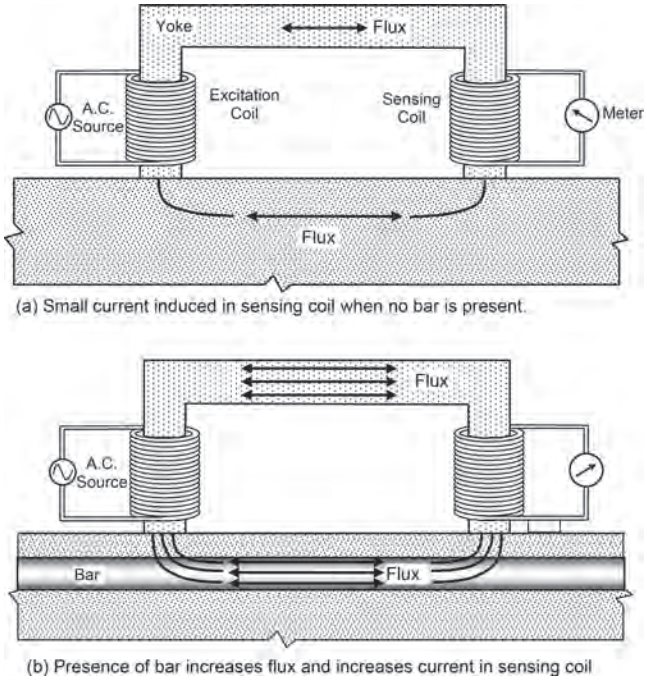

Fig. 3.5.1.1—Covermeter based on principle of magnetic reluctance (adapted from Carino [1992]): (a) small current induced in sensing coil when no bar is present; and (b) presence of bar increase current in sensing coil.

Figure 3.5.1.1 is a simplified schematic of a covermeter based on changes in the reluctance of a magnetic circuit caused by the presence or absence of a bar within the vicinity of the search head. The search head is composed of a ferromagnetic U-shaped core (yoke), an excitation coil, and a sensing coil. Note that while modern covermeters may not use exactly the type of core shown in Fig. 3.5.1.1, the basic principle of operation is the same. When alternating current (less than 100 Hz) is applied to the excitation coil, an alternating magnetic field is created and there is a magnetic flux between the poles of the yoke. In the absence of a bar (Fig. 3.5.1.1(a)), the magnetic circuit, composed of the yoke and the concrete between ends of the yoke, has a high reluctance and the amplitude of alternating magnetic flux between the poles is small. The alternating flux induces a small, secondary current in the sensing coil. If a ferromagnetic bar is present (Fig. 3.5.1.1(b)), the reluctance decreases, the magnetic flux amplitude increases, and the sensing coil current increases. Thus, the presence of the bar is indicated by a change in the output from the sensing coil. For a given reinforcing bar, the reluctance of the magnetic circuit depends strongly on the distance between the bar and the poles of the yoke. An increase in concrete cover increases the reluctance and reduces the current in the sensing coil. If the meter output was plotted as a function of the cover, a calibration relation-